Structure and mechanics of single biomolecules: experiment and simulation

2002 J. Phys.: Condens. Matter 14 R383

(http://iopscience.iop.org/0953-8984/14/14/202)

INSTITUTE OF PHYSICS PUBLISHING JOURNAL OF PHYSICS: CONDENSED MATTER

J. Phys.: Condens. Matter **14** (2002) R383–R414 PII: S0953-8984(02)17810-6

TOPICAL REVIEW

Structure and mechanics of single biomolecules: experiment and simulation

Richard Lavery[1], Anne Lebrun[1], Jean-François Allemand[2,3], David Bensimon[2] and Vincent Croquette[2]

[1] Laboratoire de Biochimie Théorique, CNRS UPR9080, Institut de Biologie Physico-Chimique, 13 rue Pierre et Marie Curie, 75005 Paris, France
[2] Laboratoire de Physique Statistique, CNRS UMR8550 Ecole Normale Supérieure, 24 rue Lhomond, 75231 Paris, France
[3] Laboratoire Pasteur, CNRS UMR8640, Ecole Normale Supérieure, 24 rue Lhomond, 75231 Paris, France

Received 1 February 2002
Published 28 March 2002
Online at stacks.iop.org/JPhysCM/14/R383

Abstract

One of the main goals of molecular biology is to understand the structure of biomolecules. With the emergence of single molecule manipulation techniques that structure can now be controlled by the application of stretching and torsional stresses. In this article we review some recent experiments on the stretching and twisting of single biopolymers, testing the elastic properties of DNA and proteins and studying their stress-induced structural transitions. Numerical simulations have emerged as a precious tool to interpret the experimental data and predict the associated structural changes. We shall explain how a combination of these experimental and computational tools open a new vista on the structure of biomolecules.

(Some figures in this article are in colour only in the electronic version)

1. Introduction

Over the past few years, biophysicists have been using single-molecule micromanipulation techniques to study the behaviour of individual biopolymers such as DNA, RNA and proteins. At a purely physical level, such experiments have provided new data against which to test models of polymer elasticity with or without specific types of interaction, such as electrostatic, self-avoidance or hybridization. It is expected that such experiments will eventually provide quantitative constraints to more complex polymer problems such as protein folding. The biological impact of these studies is reflected in the fact that the mechanical behaviour of nucleic acids and proteins turns out to be a fundamental aspect of their biological function. Consider, for instance, the double-helical structure of DNA. This structure hides the genetic content of the molecule within the core of the double helix, thus preventing easy access by proteins to the genetic code. Since the elucidation of the structure of DNA in 1953, it has

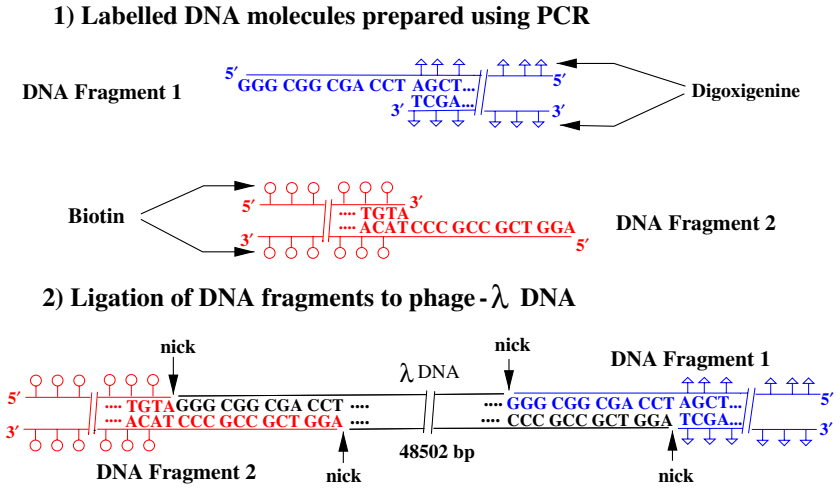

Figure 1. Schematic representation of a DNA construct. A segment of photochemically labelled DNA is fixed to each end of a 48.5 kb phage λ DNA. A 5 kb fragment tagged roughly every 200–400 bp with a biotin label is annealed and ligated to the cohesive-left end of the λ DNA. A 6 kb fragment is similarly tagged with digoxigenin molecules, and then annealed and ligated to the cohesive-right end of the phage λ DNA. The final construct, measuring about 20 μm, is biochemically labelled over 20% of its length.

become increasingly clear that the initial steps of many fundamental biological processes (such as DNA replication and the transcription of DNA into messenger RNA) depend on the unwinding, or melting, of regulatory DNA sequences. Once DNA has been locally opened by a combination of mechanical and enzymatic effects, proteins can read and copy the genetic code. As we shall also see in this review, the use of single-molecule techniques has made it possible to quantitatively reproduce and analyse such effects, leading to a much better understanding of the structural transitions which play a role *in vivo*.

In less than a decade, a wealth of new techniques and tools for the physical study of single molecules has emerged. Methods as diverse as optical and magnetic tweezers, microfibres and atomic force microscopy (AFM) are now used in many laboratories to manipulate (displace, stretch or twist) single biomolecules (DNA, proteins, polysaccharides etc).

These experiments and their interpretation in structural and mechanical terms are the focus of this review; we consequently describe the techniques involved, and present the various models used to describe biomolecules under tension and torsion and discuss their adequacy with respect to the experimental results.

Most biomolecules (DNA, RNA and proteins) are polymers, i.e. they consist of a linear chain made of repeating structural units. For proteins the building blocks are peptides, which can carry 20 different side chains forming the 20 common amino-acids. In contrast with DNA, whose double-helical structure is largely independent of its sequence, the three-dimensional structure of proteins and some RNAs (tRNA and rRNA), and consequently their function, is apparently uniquely determined by their sequence. The prediction of that structure from a knowledge of the sequence has emerged as the central goal of the post-genomic area.

The possibility to manipulate biomolecules opens a new perspective. By applying forces to these molecules they can be deformed and induced to adopt new structures. Studying these transitions will undoubtedly advance our understanding of the relation between sequence, structure, mechanics and dynamics.

2. Experimental approaches

2.1. The chemistry of trapping single molecules

To manipulate a single molecule one needs to catch the molecule by its extremities. For each type of molecule studied different strategies are available.

For DNA the most popular tools developed by biochemists are the ligand–receptor pair biotin–streptavidin and the antigene–antibody pair digoxigenin–antidigoxigenin. Modified nucleotides linked to biotin and digoxigenin are commercially available and can be incorporated in a DNA fragment using the PCR technique (photolabelling can also be used) [1–3] (see figure 1). It is then possible to obtain pieces of DNA that can bind specifically to a streptavidin- or antidigoxigenin-covered substrate. As two DNA molecules cut with the same restriction enzymes can be ligated it is possible to add labelled extremities to an unmodified piece of DNA. It is then possible to catch it by its extremities. Another possibility is to use a DNA molecule synthesized with thiols at its extremites. As thiols react spontaneously with gold, while DNA does not, it is possible to attach a DNA molecule to a gold-covered surface [4].

For RNA manipulations people have 'simply' incorporated a piece of RNA in a DNA molecule that they caught with the previously described techniques [5].

With proteins the presence of reactive chemical groups (amino for example) allow for chemical binding. If the reactant can react with another group fixed on a surface (for example another amino group covalently linked to a glass surface) the reactant can form a covalent bridge between the molecule studied and the substrate. Another way is to make a fusion protein containing the native protein and a histidine (or biotine) tail which can bind specifically to appropriately coated surfaces.

A simpler, although less controlled, way is to use nonspecific physical interactions with a substrate (see [6] for example). If a molecule can nonspecifically adhere to a surface and if the interactions are not strong enough to capture all the molecule, a part of it may be pulled. In this case the free end-to-end distance of the molecule has to be determined for each molecule.

A similar technique has been described for DNA. The interaction of DNA with a great variety of substrates obeys the following scenario: at low pH there is a strong, nonspecific interaction all along the molecule. At high pH there are no detectable interactions. Between these two regimes (at a specific pH that depends on the nature of the substrate on which DNA adsorbs) the nonspecific interactions between DNA and substrate are limited to the molecule's extremities [7]. These interactions lead to a specific anchoring of DNA by its extremities that has been used to pull on DNA molecules [8]. As we shall see later, this also provides a very simple way of aligning DNA molecules on a substrate, which can be used for their physical mapping.

2.2. Forces at the molecular scale

Let us discuss the range of forces encountered at the molecular level. The smallest force on a molecule is determined by the Langevin force f_n due to thermal agitation. This sets the lower limit for force measurements and is due to Brownian fluctuations (of energy $k_B T = 4 \times 10^{-21}$ J $= 0.6$ kcal mol^{-1}—at room temperature) of the object of size d (sensor, cell or membrane) anchored by the molecule. For a $d = 2$ μm diameter bead or cell in water (viscosity $\eta = 10^{-3}$ P), $f_n = \sqrt{12\pi k_B T \eta d} \sim 10$ fN Hz$^{-1/2}$ (note that this is a noise density, i.e. the faster the measurement, the more noisy it is). This can be compared with the typical weight of a cell, $\sim$10 fN, i.e. every second a cell experiences a thermal knock equal to its weight!

Just above these forces lie the entropic forces that result from a reduction of the number

of possible configurations of the system consisting of the molecule (e.g. protein or DNA) and its solvent (water and ions). As an example, a free DNA molecule in solution adopts a random coil that maximizes its configurational entropy [9]. Upon stretching, the molecular entropy is reduced so that at full extension there is only one configuration left: a straight polymer linking both ends. To reach this configuration, work against entropy has to be done; a force has to be applied. The entropic forces are rather weak. Since the typical energies involved are of the order of k_BT and the typical lengths are of the order of a nanometre, entropic forces are of the order of k_BT nm^{-1} = 4 pN (4×10^{-12} N). These are typically the forces exerted by molecular motors, such as myosin on actin [10], the force necessary to stretch a DNA molecule to its contour length [3] or to unzip the two strands of the molecule [11, 12] (although in this case entropic energies are only part of the total free energy change).

Noncovalent (e.g. ligand/receptor) bonding forces are much stronger. They usually involve modifications of the molecular structure on a nanometre scale: breaking and rearrangement of many van der Waals, hydrogen, or ionic bonds and stretching of covalent bonds. The energies involved are typical bond energies, of the order of an electron-volt (1 eV = 1.6×10^{-19}J = 24 kcal mol^{-1}). The elastic forces are thus of the order of eV nm^{-1} = 160 pN. These are typically the forces necessary to break receptor–ligand bonds [13–17] or to deform the internal structure of a molecule [2, 18, 19].

Finally the strongest forces encountered at the molecular scale are those required to break a covalent bond of the order of 1 eV Å^{-1} $\sim$ 1600 pN.

Since the range of forces of interest spans several decades, different instruments are necessary to cover the full range.

2.3. Techniques for manipulating single molecules

There are already many techniques to manipulate single molecules: atomic force cantilevers [13], microfibres [2,20], optical [21] or magnetic tweezers [22,23] and traps [1,18], hydrodynamic drag [3] and biomembrane force probes (BFP) [24]. In all these techniques, a molecule (DNA, protein or some other polymer) is first anchored to a surface at one end and to a force sensor at the other. The force sensor is usually a trapped micrometre-sized bead or a cantilever, the displacement of which is used to measure the force (figure 3). Thus for an AFM cantilever (or a microfibre) of known stiffness the force is proportional to its measured bending.

2.3.1. Optical tweezers. Like a dipole attracted by a high electric field, a bead with a permittivity higher than its surroundings can be trapped at the focal point of a focused laser beam.

By using two co-axial counter-propagating laser beams a small transparent bead can be trapped with a force of $\sim$100 pN. The force exerted on the bead can be deduced from the displacement of the trapping beam due to its refraction in the bead, i.e. by directly measuring the momentum transfer [25]. This absolute measure bypasses the need for a calibration of this optical trap.

A slightly different technique, based on the same principles, uses a single intensely focused laser beam (optical tweezers, [21]) to hold a transparent bead of radius r of $\sim$1 μm. Forces ($F < 50$ pN) can be measured by following the displacement δx of the bead from its equilibrium position: $F = k_{trap}\delta x$. The optical trap stiffness k_{trap} has to be determined prior to any force measurement, for example by pulling on the bead with a known force such as the hydrodynamic drag F_s of a fluid (of viscosity η) flowing with a velocity v around the bead: $F_s = 6\pi\eta r v$. Alternatively, one may determine k_{trap} by measuring the intensity of the Brownian fluctuations

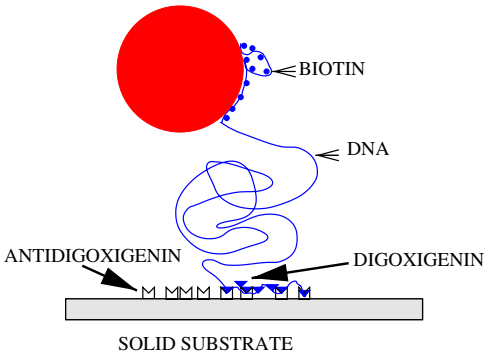

Figure 2. To attach a single DNA molecule, biotin-labelled bases are incorporated at one end so that this extremity can bind to a streptavidin bead while the second extremity is labelled with digoxigenin, which can bind to antidigoxigenin adsorbed on a solid substrate (see figure 1). The bead can be trapped in optical tweezers or in a magnetic field if it is superparamagnetic. The solid substrate can be a pipette or a glass surface.

$\langle \delta x^2 \rangle$ of the trapped bead. By the equipartition theorem these satisfy [21, 26, 27]

$$\frac{k_{trap}\langle \delta x^2 \rangle}{2} = \frac{k_B T}{2}. \tag{1}$$

2.3.2. Biomembrane force probe. The BFP is a technique pioneered by Evans [24]. It consists of using the deformation of a 10–20 μm vesicle under tension as a force sensor. The tension in the vesicle is controlled by a suction pipette that sets the hydrostatic pressure difference across its membrane. The advantage of this technique is that the stiffness of the force sensor (i.e. the tension) can be set at will, allowing for the measurement of a very large range of forces (from 10^{-15} to 10^{-9} N). This method has been used to monitor the force required to break bonds between receptor–ligand, antigen–antibody etc pairs.

2.3.3. Magnetic tweezers. To twist and stretch a DNA molecule and study its interactions with proteins, a magnetic trapping technique [1] has proved particularly convenient (figure 2). Briefly, it consists of stretching a single DNA molecule bound at one end to a surface and at the other to a magnetic microbead (1–4.5 μm in diameter) (see figure 3). Small magnets, whose position and rotation can be controlled, are used to pull on and rotate the microbead and thus stretch and twist the molecule. This system allows one to apply and measure forces ranging from a few femtonewtons (10^{-3} pN) to nearly 100 pN (see [28]) with a relative accuracy of $\sim$10%. In contrast with some other techniques, this force measurement is absolute and does not require a calibration of the sensor. It is based on an analysis of the Brownian fluctuations of the tethered bead, which is completely equivalent to a damped pendulum of length $l = \langle z \rangle$ pulled by a magnetic force F (along the z-axis). Its longitudinal ($\delta z^2 = \langle z^2 \rangle - \langle z \rangle^2$) and transverse ($\delta x^2$) fluctuations are characterized by effective rigidities $k_\parallel = \partial_z F$ and $k_\perp = F/l$. By the equipartition theorem they satisfy [26, 27]

$$\delta z^2 = \frac{k_B T}{k_\parallel} = \frac{k_B T}{\partial_z F} \tag{2}$$

$$\delta x^2 = \frac{k_B T}{k_\perp} = \frac{k_B T l}{F}. \tag{3}$$

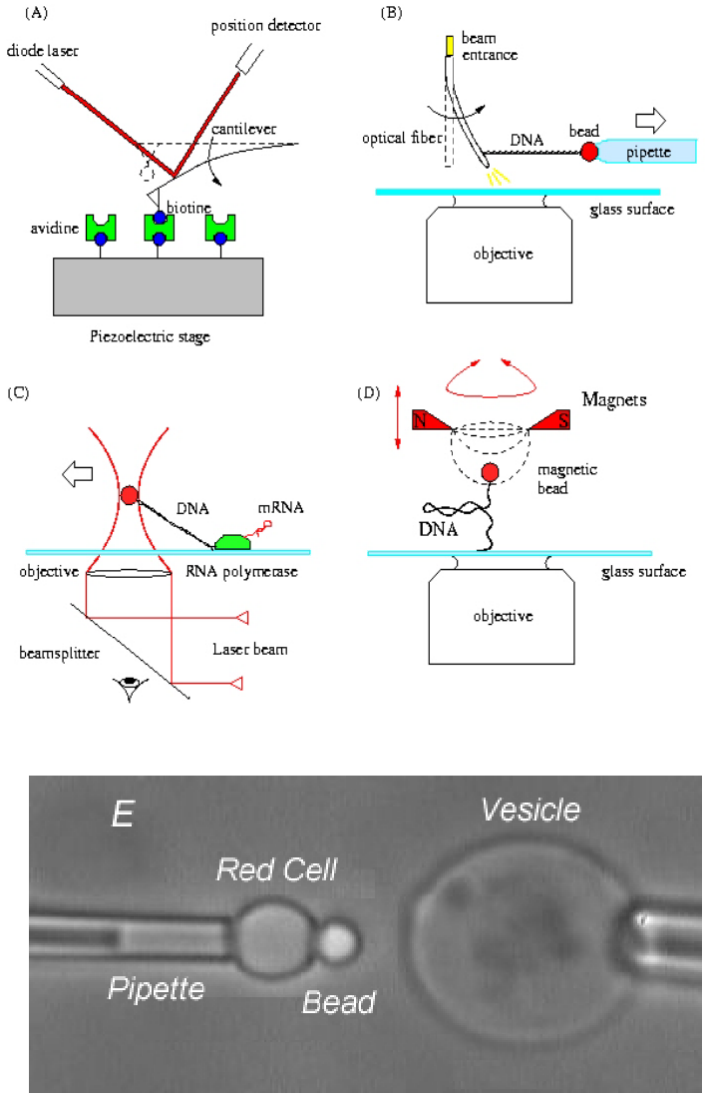

Figure 3. Example of force transducers. (*a*) An AFM cantilever is often used as a force transducer during intermolecular force measurements [13] and protein unfolding experiments [33]. Its deflection upon pulling is detected by the displacement of a laser beam reflected from the cantilever.(*b*) In some of the experiments involving DNA pulling [2,34] and unzipping [11], the force transducer is an optical fibre, whose deflection is detected optically (by measuring the displacement of either the fibre directly on a microscope stage or of a light beam emitted from its pulled end). (*c*) A force transducer often used to characterize molecular motors [10, 21, 35] is optical tweezers which consist of a single strongly focused laser beam holding a bead at its focal point. The displacement of the bead in the trap is observed with a microscope and, together with the trap stiffness, is used to assess the trapping force. (*d*) Small magnets can be used to pull and twist a DNA molecule tethering a superparamagnetic bead to a surface. As explained in the text, in this case the force can be deduced from the amplitude of the Brownian fluctuations. (*e*) A small vesicle held in a micropipette by controlled suction can be used as a force probe. A small bead stuck to this vesicle carries a ligand whose interaction with receptors on a nearby cell can be deduced from the deformation of the membrane under tension. Since the stiffness of the sensor is set by the pressure difference across the membrane, a particularly large force range is accessible by this method. (This illustration was kindly provided by Pincet and Perez.)

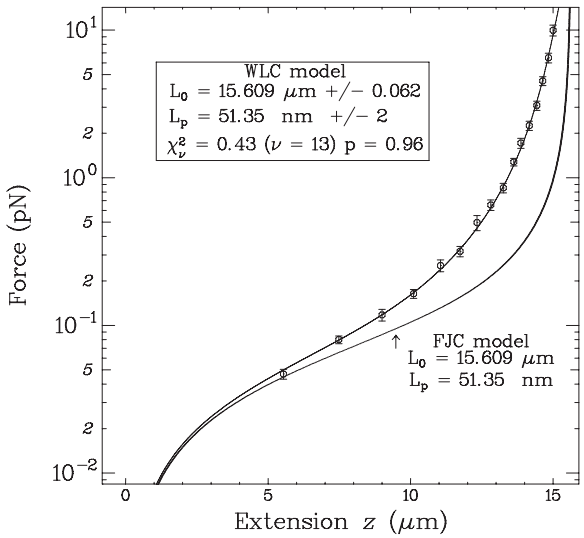

Figure 4. Experimental data and fit corresponding to the extension of a λ DNA molecule in 10 mM PB buffer obtained using the Brownian motion method. The logarithmic scale allows a large force range to be covered. The WLC model (full curve) fits the experimental data very nicely; we have drawn the FJC model for the same persistence length and contour length.

Thus from the bead's Brownian fluctuations (δx^2, δy^2) one can extract the force pulling on the molecule (the smaller the fluctuations the greater F) and from δz^2 one obtains its first derivative, $\partial_z F$. This measurement method can be used with magnetic (but not optical) traps because the variation of the trapping gradients occurs on a scale $\sim$1 mm, much larger than the scale on which the elasticity of the molecule changes, $\sim$0.1 μm. In other words, the stiffness of the magnetic trap is very small compared with F/l. A further bonus of the magnetic trap technique is that measurements on DNA at constant force are trivial (by simply keeping the position of the magnets fixed). With cantilevers or optical tweezers, working at constant force requires an appropriate feedback to ensure that the displacement of the sensor is kept constant. Moreover magnetic traps (and microfibres) allow very simple twisting of the molecule by rotating the magnets (or the fibre pulling on the DNA). However, because its stiffness depends on the force, the magnetic trap technique has at weak forces ($<$1 pN) a spatial resolution of $\sim$10 nm, lower than the other manipulation methods. Finally, note that by using electro-magnets, a faster and more versatile magnetic tweezers system has recently been developed [23].

2.3.4. AFM and glass microneedle. These techniques use the deflection of a mechanical spring to measure a force.

Glass microneedles [29, 30] have a typical stiffness of about 10^{-5} N m^{-1} [11, 31]; with a 10 nm resolution of the fibre's displacements [11] one could measure forces in the range of tens of femtonewtons. However, the large size of the glass fibre imposes a relatively large Langevin force, of the order of 0.5 pN Hz$^{-1/2}$. Fast measurements made by sampling between 10 and 100 Hz therefore limit the force measurement to a resolution of a few piconewtons. In the case of an AFM cantilever with a typical stiffness of 10^{-3} N m^{-1} [32], a spatial resolution at the angstrom level should allow for the measurement of forces as low as 1 pN. Once again, however, the Langevin force acting on the cantilever is large, of the order of 0.1 pN Hz$^{-1/2}$ for

high-quality cantilevers, and rapid measurements made with these instruments are typically limited to a resolution of about 10 pN.

2.3.5. Comparison between these techniques. In the case of optical tweezers, one generates a trap with a minimum stiffness of about 10^{-5} N m^{-1}, but the trap's dimensions are small, of the order of 0.5 μm. This corresponds to forces of the order of piconewtons. To generate higher forces with possible adverse effects on the molecules studied, one needs to increase the laser power. If the power is too low, the trapping potential is too weak and does not function effectively. The spatial resolution of the bead's position within the trap can be of the order of a few angstroms, implying that one should be able to measure forces as small as a few femtonewtons. Once again though, the thermal forces acting on the bead hinder the measurement of such low forces, and for a bead with a micrometre-scale diameter the limiting thermal resolution is about 10 fN Hz$^{-1/2}$. Fast experiments performed with a bandwidth of a few hundred Hertz thus cannot measure forces much lower than 0.1 pN. Unfortunately, if one attempts to reduce the noise by reducing the bead size, one obtains a weaker trapping potential.

Magnetic tweezers, using roughly the same sensor—a small bead—experience similar thermal limitations. With magnetic tweezers however, the trapping potential can be reduced until the bead's weight (or buoyancy) becomes apparent. At this point, decreasing the bandwidth allows for precise force measurements. Another advantage of magnetic tweezers is that they represent the only natural force clamp in the micromanipulation toolbox. Optical tweezers, glass fibres and AFM cantilevers are natural extension clamps, but they can be converted to force clamps by using feedback loops.

3. Theoretical approaches

Force experiments on single biological macromolecules yield important information on structure-related mechanical properties, but do not themselves yield direct data on the atomic-level conformational changes induced by the mechanical work. The coupling between the measured forces and the molecular structure can be deduced from theoretical models at various degrees of detail.

3.1. Polymer physics models

In the low-force regime ($F < 10$ pN), the elastic behaviour of DNA has an entropic origin. As the result of thermal fluctuations, DNA, like any polymer in solution, bends and curves locally, shortening the end-to-end distance of the molecule. The resulting elastic behaviour can be described by two models [1, 3, 18, 28, 36–40]: the freely jointed chain (FJC) and wormlike chain (WLC) models.

The simplest elasticity model used to describe polymers is the FJC model, where each monomer corresponds to a unitary segment b whose orientation is completely independent of its neighbour's. Under a stretching force ($\vec{F}$), such a segment is equivalent to a spin in a magnetic field, the entire polymer length being equivalent to the magnetization of a paramagnetic substance in a magnetic field. On one hand, the system likes to align itself with the force, thus gaining an energy Fb. On the other hand, it wants to adopt a random orientation in order to maximize its entropy. As expected, the competition between the two regimes will depend upon the ratio Fb/k_BT. For small forces ($F < k_BT/b$), the polymer adopts a random coil configuration, and its end-to-end extension is small. For large forces, the polymer is nearly

completely stretched. The extension versus force curve is described by the Langevin function:

$$\frac{l}{l_0} = \coth\left(\frac{F\,b}{k_B T}\right) - \frac{k_B T}{F\,b}. \tag{4}$$

The length b is called the Kuhn length and is equal to twice the persistence length (ξ, the distance over which the orientational correlation decreases by a factor of e). For DNA, the persistence length is large compared with the distance between two bases: $\xi \sim 50$ nm. As can be seen in figure 4, though adequate at very low forces, the FJC model does not fit the elastic behaviour of DNA over the whole entropic regime.

A much better description of the elastic behaviour of DNA in its entropic regime is provided by the WLC model (the continuous curve in figure 4 fits the data very well over three decades in force). This model describes a DNA molecule as a semi-flexible polymer chain of length l_0 and bending modulus B (or persistence length $\xi = B/k_B T$). The energy E_{WLC} of a given configuration $\vec{t}(s)$ of a molecule stretched by a force F along the z-axis is

$$E_{WLC} = \frac{B}{2}\int_0^{l_0}\left(\frac{\partial \vec{t}(s)}{\partial s}\right)^2 \mathrm{d}s - F\int_0^{l_0}\vec{t}(s)\cdot\vec{z}\,\mathrm{d}s \tag{5}$$

where $\vec{t}(s)$ is the local tangential vector at curvilinear coordinate s along the molecule. The first term is the bending energy, while the second sets the extension l of the molecule: $0 < l < l_0$. A detailed analysis of this model, which is beyond the scope of this review, can be found in [37, 39]. Although the force versus extension behaviour can be computed to any desired accuracy, a convenient and very accurate approximation (within 0.1%) is

$$\frac{F\xi}{k_B T} = x - \frac{1}{4} + \frac{1}{4(1-x)^2} + \sum_{i=2}^{7} a_i x^i \tag{6}$$

where $x = l/l_0$ is the relative extension of the molecule and $a_2 = -0.516\,4228$, $a_3 = -2.737\,418$, $a_4 = 16.074\,97$, $a_5 = -38.876\,07$, $a_6 = 39.499\,44$, $a_7 = -14.177\,18$ [39]. Fitting the force versus extension data to this theoretical prediction yields the most accurate estimate of the DNA's persistence length ξ and allows the study of its dependence on ionic conditions [41].

Beyond the entropic regime, i.e. from ~6 to about 70 pN, DNA behaves like an elastic rod with stiffness $EA \sim 1000$ pN [18] (where E is the Young modulus of DNA and A its effective cross-sectional area [42]). Neglecting entropic contributions, the force versus extension curve follows a simple Hookean law: $F = EA(x-1)$ (with $x > 1$). Notice that there exist some *ad hoc* formulae interpolating between the entropic and Hookean regimes, for example replacing the term $(1-x)^2$ in equation (6) by $(1 - x + F/EA)^2$ [40]. At ~70 pN, DNA undergoes a structural phase transition, which is best understood with atomic-scale models.

3.2. Atomic-scale models

In order to understand the details of conformational change under applied force, it is necessary to move to atomic scale models. Given that both nucleic acid fragments and proteins typically contain thousands of atoms, it is currently impossible to model such macromolecules using quantum mechanical techniques. The problems posed by such systems are compounded by the fact that biomacromolecules are polyelectrolytes, whose structures are strongly dependent on the environment (solvent, salt concentration, pH, ...) and are also only marginally stable.

Atomic-scale modelling currently relies upon classical force fields which have been formulated and parametrized on the basis of experimental data and quantum chemical calculations to reproduce both the structural and dynamic behaviour of biomacromolecules.

Such force fields are typically composed of so-called bonded terms representing the, generally harmonic, deformation energy associated with bond stretching and valence angle deformation, as well as the energy penalties for rotation around single bonds, and so-called nonbonded terms which account for the electrostatic and Lennard-Jones (short-range repulsion and dispersion) interactions between more distant atoms. While such force fields can describe conformational changes relatively well, they are clearly not applicable to chemical processes such as bond breaking, bond formation, electron transfer or, generally, the description of electronically excited states. It should also be noted that effects such as electronic polarization are absent from most current force fields, mainly due to the associated computational costs. Similar restrictions also applied, until recently, to nonbonded terms, which, in principle, act between all pairs of atoms within the system studied. This is not a problem for short-range Lennard-Jones terms, but generally required the arbitrary truncation of electrostatic interactions, which only decrease as the inverse of the distance separating the atoms. This turned out to be particularly problematic for the highly charged nucleic acids. Happily, such difficulties can now be avoided, notably in the case of simulations using periodic boundary conditions, via techniques based on Ewald lattice-sums [43].

The effort implied by force field development has tended to reduce the number of groups working in this area and has concentrated resources on a small number of general purpose force fields. The reader is refer to articles dealing with the latest versions associated with the molecular simulation programs AMBER [44], CHARMM [45] and GROMOS [46], which are most commonly used in the biomolecular field.

In order to represent the solvent and counterions which surround biomacromolecules in their natural environment, it is usual to maintain an atomic-scale representation. This implies imbedding the macromolecule in a droplet of several thousand water molecules (and, to reproduce physiological salt concentrations, severals tens of counterions). To avoid surface-related effects, it is also common to use periodic boundary conditions, in which case the solvent-enveloped macromolecule is placed in a rectangular or octahedral cell surrounded by a layer of identical cells. It should be noted that the addition of explicit solvent molecules and counterions leads to systems typically involving tens of thousands of atoms.

Alternative approaches attempt to reproduce environmental effects using continuum models. The simplest approach in this area replaces the dielectric constant in the Coulomb equation with an empirical distance-dependent function which attempts to account for microscopic effects on electrostatics. Such functions, which can be either linear or sigmoidal functions of the distance separating interacting charges, allow for stronger interactions at short range, while approaching the dielectric damping due to the bulk solvent at long range. An important element missing from such approaches is the variation of damping related to the distance of charges from the solvent interface. This problem can be corrected by using formulations based on the Poisson–Boltzmann model with a defined interface between the high-dielectric solvent and the low-dielectric macromolecule. Again, computational costs require some simplifications, and a number of groups are now working on so-called generalized Born models [47,48], which reproduce well Poisson–Boltzmann electrostatic energies, but are only beginning to be applied to biomolecular simulations.

Once the force field and environmental representation has been defined, a simulation method must be selected. In the case of explicit solvent representations, molecular dynamics (MD) is the natural choice. Algorithms for MD have been refined over several decades and can be used effectively on multiprocessor computers. Dynamic simulations rely on numerical integration of Newton's equations of movement, with each atom in the system having three degrees of freedom in Cartesian space. Consequently, the integration time-steps are bounded by the fastest movements occurring in the system, notably the vibration of bonds

to light hydrogen atoms, whose characteristic movements occur on the femtosecond timescale. Usual time-steps are thus 1–2 fs, which, given current computer power, imply that the duration of MD simulations for macromolecular systems are typically limited to several nanoseconds. Simplified solvent representations, or the use of restraints on the fastest movements in the systems can improve the situation, but currently represent a gain little more than a factor of ten.

An alternative approach involves using energy minimization. This is however impractical with either Cartesian atomic variables, or explicit solvent representations, where the conformational space to be searched has tens of thousands of dimensions and a vast number of local energy minima. Successful minimizations require simpler internal coordinate models for the macromolecule (freezing degrees of freedom associated with higher deformations energies such as bond stretches or angle bends) coupled with implicit solvent/counterion representations. Such approaches, which are the subject of a recent review [49], have been used to look at the structural consequences of applied forces on both nucleic acids [2, 19, 50] and proteins [51]. In the case of energy minimization, geometrical restraints are used to represent the effects of applied forces and slowly modifying these restraints allows a deformation pathway to be defined over the enthalpy surface in conformational space. In the case of MD, a force can be applied to the macromolecule (or to a ligand bound to a macromolecule) via a harmonic spring [52–56], or the effects of a force can be mimicked by biasing the atomic velocities of the constrained atoms during the evolution of the dynamic trajectory [57]. In either case, deformations which take into account the effect of thermally induced fluctuations can be studied. However, due to the time limitations mentioned above, these deformations must be created on a nanosecond timescale, and thus many orders of magnitude faster than in the laboratory experiments. A number of studies have addressed the changes in the force profile which result from changing loading rates, as well as the recovery of data on the underlying free-energy surface from studies carried out at different loading rates [58–60]. It is lastly remarked that although algorithms for obtaining free-energy variations from MD simulations exist, they are generally difficult to apply to the large-scale deformations created during single-molecule experiments [61]. Recent approaches based on snapshots drawn from MD trajectories combined with simplified estimates of solvation and, eventually, entropic contributions, however, are of interest in the case of macromolecule–ligand [62] or macromolecule–macromolecule [63] interactions.

4. Studies of biopolymers

4.1. DNA

4.1.1. Stretching. Early experiments of spreading DNA on surfaces [64, 65] showed that the double helix could be stretched to roughly twice its normal contour length (figure 5). This possibility, now termed 'DNA combing', already has important biological applications, notably in DNA hybridization experiments and in studies of DNA replication [66–68]. However, since the role of DNA–surface interactions is a complicating factor in these experiments, other methods have been developed to stretch DNA molecules in solution, under physico-chemical conditions close to those prevailing within the cell. Two groups succeeded in this endeavour in 1996. Cluzel *et al* [2] used biotin–streptavidin and DIG–antiDIG interactions to fix a λ DNA 16.2 μm in length between a narrow glass fibre, which served as a force transducer, and a polystyrene microbead, which could be pulled using a micropipette mounted on a piezoelectric stage. Smith *et al* [18] attached microbeads to both ends of a λ DNA and used laser tweezers to hold one end and to pull on the other. Both groups found that, at low force, the molecule could be stretched to its contour length in accordance with predictions from the WLC model

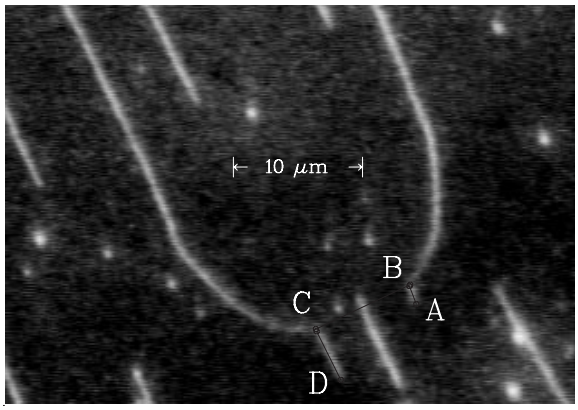

Figure 5. Fragment of genomic DNA of one of the authors combed on a hydrophobic surface. The DNA bound at both ends forms a typical broken loop. From measurements on such figures we deduce the extension of DNA at the breaking point: the stretched molecule length is $l_b = \bar{B}\bar{C}$; its unstretched length $l_{b,0}$ is deduced by dividing the length $\bar{A}B + \bar{D}C$ by the extension factor observed for a straight molecule combed on a hydrophobic surface (1 μm for 2 kb).

(overcoming the entropic resistance favouring a random coil conformation) and then extended elastically. However, at a force of roughly 70 pN, a plateau appeared in the force versus extension curve where the DNA molecule increased its length to roughly 1.7 times the normal contour length (figure 6). Beyond this point, further extension led to a rapid increase in force and to rupturing the molecular construction.

The unexpected force plateau was interpreted as a cooperative phase transition leading to a new conformation of DNA, which was termed S-DNA by Cluzel *et al*. In line with earlier suggestions of Thundat [65], Smith *et al* [18] suggested that this transition would involve helical unwinding, whereas Cluzel *et al* [2] proposed a conformation, based on restrained molecular modelling, which involved strong base inclination leading to a smaller helical diameter, but little unwinding. The cooperative nature of the transition to this model conformation was confirmed by deriving the deformation energy to obtain a force curve, which effectively showed a plateau over the same range of extensions as found experimentally (although the model plateau occurred at higher force). It was however remarked in this article that the stretched conformation of DNA depended on how the molecule was constrained and could also be influenced by sequence effects. This dependence was shown explicitly in subsequent studies [19] which used internal coordinate molecular modelling to demonstrate that pulling on the two 5′-ends of a duplex resulted in the narrow fibre form with inclined bases and little unwinding, while pulling on the 3′-ends led to an unwound ladder-like conformation (see figure 7). This dependence on the manner of stretching the molecule was supported by other theoretical studies using MD [61,69]. Similar results were also obtained by Kosikov *et al* [50] with a molecular mechanics approach, although their structures cannot be classified in the same way since the helical rise, rather than end-to-end distances, was used as the restraint variable. Concerning base sequence effects, the work of Lebrun and Lavery [19] showed that AT-rich sequences could be extended more easily that GC-rich sequences (in line with later studies of DNA oligomers using AFM, [6]) and suggested that the deformation energy for creating the fibre form of S-DNA was smaller than that necessary to create the ribbon form. The latter result is linked mainly to base stacking, which is better conserved in the fibre form. It should be added that base stacking appears to play a major role in the cooperativity of the stretching transition, since it is the principal factor

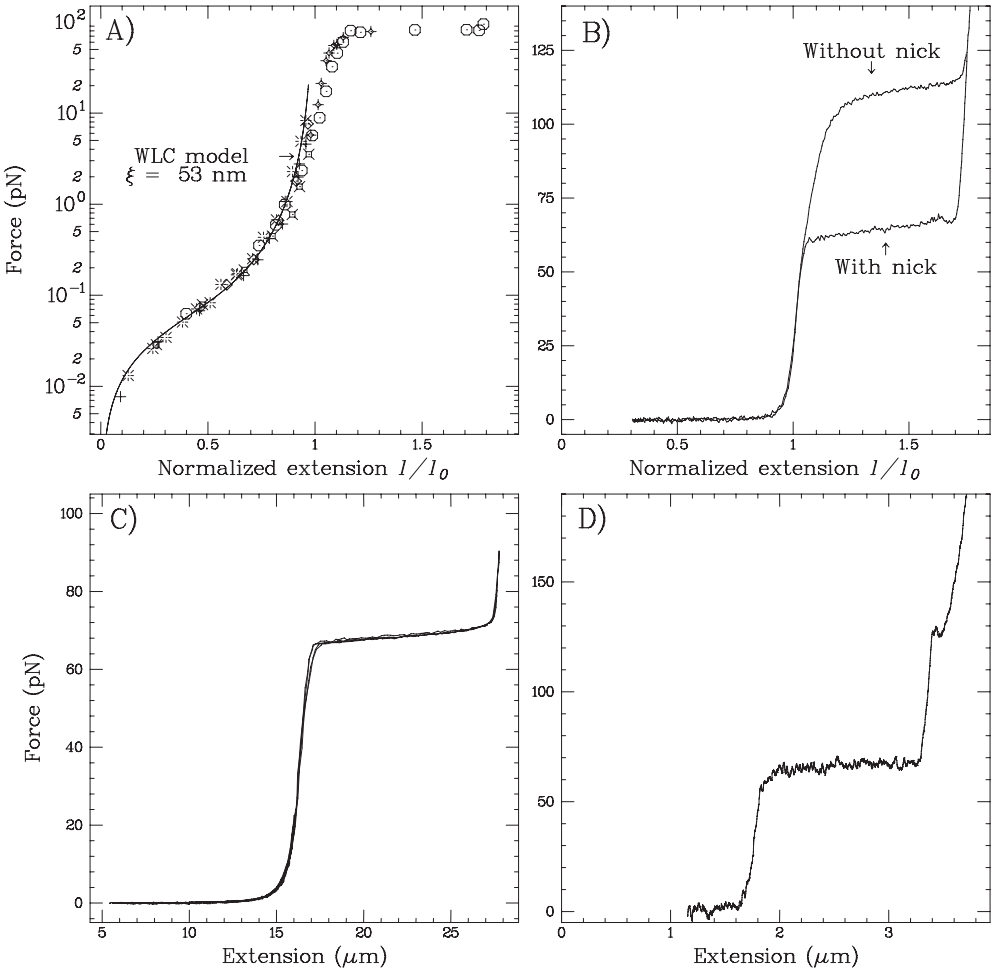

Figure 6. Force versus extension curves of single DNA molecules obtained by different groups. (*a*) The points correspond to several experiments performed over a wide range of forces. The force exerted by small magnets placed above the sample was measured using the Brownian fluctuation technique described in the text [1]. At high forces, the molecule first elongates slightly, as would any material in its elastic regime. Above 70 pN, the length abruptly increases, corresponding to the appearance of a new structure called S-DNA. (*b*) The same transition observed by Léger and Chatenay using a glass needle deflection on a nicked molecule (i.e. containing single-strand breaks) and an un-nicked molecule (the transition occurs for a higher force). (*c*) The transition is also observed by Smith and Bustamante using optical tweezers. (*d*) Finally, Clausen-Schaumann and Gaub also observe the transition using an AFM.

disfavouring junctions between the stretched and unstretched forms of the double helix (see also [70]).

The actual conformation of S-DNA is still under study (see figure 7). Early data in favour of the inclined base, fibre-like form comes from the experiments of Wilkins on stretched DNA fibres [71], where spectroscopic results were compatible with base pair inclination. These experiments have been repeated recently, profiting from the much higher x-ray intensities now available. The results again favour the fibre model by showing that the stretched fibres yield a hexagonal lattice spacing of only 1.3 nm, compared with the normal DNA diameter of roughly

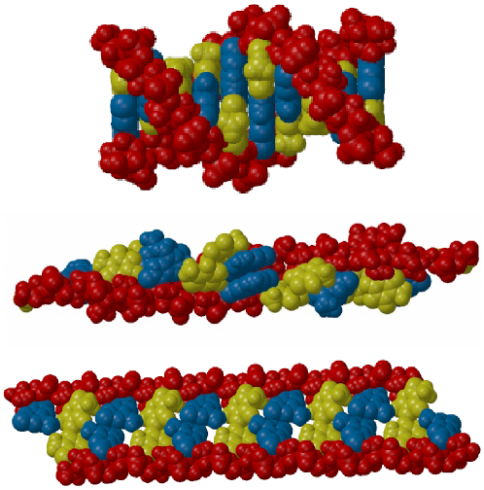

Figure 7. The new structures of DNA obtained in numerical simulations when pulling on the molecule. Top: usual B-DNA structure; center: if the molecule is pulled by its 5′ ends, it keeps a double helical structure with tilted bases; bottom: if the DNA is pulled by its 3′ extremities the final structure resembles a ladder.

2.0 nm [72]. On the other hand, more refined micromanipulation experiments, which were able to constrain DNA rotation, led to the conclusion that S-DNA has a residual twist between base pairs of only 9°–10° [73]. AFM studies have also indicated that constraining DNA unwinding during stretching leads to a less cooperative transition at higher force [74]. It should be added that theoretical work by Williams and collaborators [75] has led to a completely different interpretation of the stretching experiments, where the proposed B–S transition is replaced with DNA melting. This difference in the behaviour of overstretched B-DNA could be due to the existence of nicks in the molecule leading to melting concomitant with the transition to S-DNA.

More recent micromanipulation experiments of DNA stretching have aimed at explaining ionic strength effects and have notably enabled studies of DNA condensation induced by multivalent ions such as Mg^{2+} or polyamines [40, 41].

In parallel with micromanipulation experiments on polymeric DNA molecules, other groups have investigated DNA mechanics using AFM. This technique, used already in 1995 by Boland and Ratner [76] to investigate base–base interactions, is adapted to studying short DNA fragments, ranging from a few tens up to roughly one thousand nucleotides. This opens up the possibility of studying sequence specific effects using synthetic DNA fragments, which is impractical for long DNA molecules. The early studies of Lee *et al* [17] made use of this possibility to investigate the binding of an $(ACTG)_5$ strand to the AFM tip and its complementary $(CAGT)_5$ strand bound to a silica surface. Both strands were attached via thiol labels at their 5′-extremities. Upon bringing the tip closer than 5 nm to the surface, an attractive interaction was detected and, by then withdrawing the tip, it was possible to measure the rupture force. A histogram of the results showed three distributions centred around 1.52, 1.11 and 0.83 nN, which were interpreted as being due to the formation of duplexes with 20, 16 and 12 bp respectively. In 1997, Noy *et al* [4] carried out similar experiments with a 14-mer whose sequence, d(TCGGACAATGCAGA), was chosen so that any shift between the two strands would allow the formation of no more than two Watson–Crick base pairs. The two strands of the duplex were each tethered at their 5′-ends. Reproducible results were

achieved, with a rupture force for specific oligomer binding of 0.46 ± 0.18 nN. As with the micromanipulation experiments on polymeric DNA [2, 18], the AFM force curves showed a plateau, although at a higher force of 120 ± 50 pN, associated with DNA lengthening by roughly a factor of two before rupture occurred. Integrating the force over the distance necessary to rupture the duplex led to a binding enthalpy of 124 kcal mol^{-1}. This value is 50 kcal mol^{-1} above the estimated denaturation energy of the 14-mer, and the difference was attributed to the energy necessary to stretch of the duplex. However, it should be remarked that these experiments may suffer from nonspecific interactions between the AFM tip and the substrate and indeed studies by Strunz *et al* which used a layer of polymer (PEG) between both surfaces and the DNA oligomers led to considerably lower unbinding forces (20–50 pN for 10–30 bp). More recent AFM experiments by Rief *et al* [6] obtained force plateau values of 65 pN for λ DNA fragments, 35 pN for poly(dA–dT) and 65 pN for poly(dG–dC). It was noted that, after relaxing the separated strands of the synthetic polymers, hairpins could be formed within each strand and these hairpins could themselves be opened with forces around 20 pN. From these experiments, it was possible to calculate the rupture forces for AT and GC base pairs as 9 and 20 pN respectively, values which are in good agreement with those obtained in the Heslot group by separating the strands of polymeric DNA molecules [11, 12] and with recent laser tweezer experiments on DNA by Bustamante *et al* [77] (16 pN for a hairpin with an alternating GC sequence). Later work from the Gaub group tested both the influence of varying salt concentration [74] and chemical modification with cisplatin [78] on the stretching and rupture forces. A general finding from these AFM experiments was that, whereas duplex stretching occurs rapidly and can equilibrate during the pulling (and is thus associated with forces that are independent of the loading rate), strand separation is a much slower, and probably multi-step process—although it should be added that Strunz *et al* [79], studying 10–30 bp oligomers, have found that rupture forces vary as the logarithm of the loading rate, suggesting a single barrier process.

Several attempts were made to numerically model these experiments. Konrad and Bolonick [69] used MD and a simple continuum solvent model to pull apart an $(ACGT)_3$ duplex by its 3′-ends. In line with the molecular mechanics modelling by Lebrun and Lavery [19], this led to an unwound 'S-ladder' conformation with a maximum elongation of 2.1-fold. The force necessary for the elongation, 85 pN, and for strand separation, 0.6 nN, were in good agreement with the experimental data. MacKerell and Lee [61] studied the same oligomer, but with 5′5′ constraints, and, not unexpectedly, found that this type of stretching led to base inclination with little unwinding (at least, before strand rupture occurred). This study included potential of mean force estimates of the free energy of DNA deformation and came to the conclusion that strand separation occurred when inter-strand phosphate repulsion could not longer be balanced by solvation terms. Molecular mechanics modelling [80] of oligomer stretching using 5′5′ and 3′3′ restraints on the 14-mer sequence studied by Noy *et al* confirmed the structural results which had been obtained with polymeric DNA [19]. The 5′5′ plateau occurred at 100 pN, close to the Noy result and considerably lower than the 3′3′ plateau (250 pN). It should be noted that the force plateau in these modelling experiments was found by differentiating the energy curves, which required a polynomial fit to remove the noise associated with abrupt, local structural changes. This fitting can affect the resulting force curve. However, in a more recent study [81], the existence of a sudden lengthening of the DNA oligomer was confirmed by applying a steadily increasing force to the oligomer.

4.1.2. Twisting. DNA twisting, biologically termed supercoiling, has been harnessed in a series of single-molecule experiments [1, 28, 82, 83], which have led to a deeper understanding of how double-stranded DNA reacts to rotational torque. This area of DNA mechanics has

considerable biological importance, since DNA is generally under torsional stress within cells. The topological consequences of changing DNA twist were originally formulated by White [84] in the equation

$$Lk = Wr + Tw$$

where Lk, the linking number (a topological constant), is the number of times the single strands forming the duplex cross one another, Wr is the writhe, or the number of times the duplex crosses over itself within supercoiled loops, and Tw is the twist, or the number of helical turns within the duplex. Thus, when DNA is subjected to a change in the linking number, ΔLk, the resulting stress can be distributed between changes in the three-dimensional writhing of the molecule and internal changes of the helical twist. Experiments on DNA plasmids using gel electrophoresis [85, 86], electron microscopy [87, 88] and fluorescence depolarization studies [89] have established that DNA generally prefers writhing to changing its twist in a ratio of roughly 4:1. Biologically, supercoiling is generally characterized using a supercoiling density,

$$\sigma = \Delta Lk/Lk_0$$

where Lk_0 is the linking number of the relaxed DNA molecule. Within typical cells and viruses, σ ranges from -0.05 to -0.07. This negative supercoiling helps in packaging the DNA and is involved in both gene expression and DNA replication. Not surprisingly, a complicated enzymatic machinery, notably involving the topoisomerases and gyrases, is necessary to maintain a correct superhelical density. (It is interesting to note that many thermophilic bacteria have positively supercoiled DNA maintained by a reverse gyrase [90].)

The single-molecule experiments [1,28,82,83] which have been used to study supercoiling involved constructing a DNA molecule with functionalized ends that could be attached at multiple sites and developing a means of exerting both longitudinal force and rotational torque on the tethered molecule. λ DNA with 48.5 kb (16.2 μm in length) was used for this purpose. Roughly 1 kb end-fragments, functionalized with either DIG or biotin, were used to attach the DNA to a glass surface (coated with anti-DIG) at one end and to a superparamagnetic bead (coated with streptavidin) at the other. The molecule could then be stretched or twisted using magnets mounted above the tethered molecule (see figure 3). Changing the height of the magnet changed the force on the molecule, which could be measured by observing the Brownian fluctuations of the bead. Rotating the magnet leads to rotating the bead, as confirmed by observation through an inverted microscope, and thus to changing the twist of the DNA molecule. For n turns of the magnet one generates a $\sigma = n/Lk_0$ (where, for the present construct, given that DNA in solution has, on average, 10.5 bp/turn, Lk_0 is roughly 4660).

Two types of experiment can be carried out with this approach: moving the magnet up and down gives access to force versus extension curves, while rotating the magnet held at a constant height gives access to extension versus σ curves. Initial trials of this apparatus showed that it was possible to find beads bound to single DNA molecules without any single-strand nicks and which would consequently react to torsional stress [1]. It was found that, for small applied forces ($F < 0.45$ pN for negative supercoiling; $F < 3.0$ pN for positive supercoiling), twisting the DNA led to a reduction in the apparent length of the molecule due to writhing and the formation of plectonemes (like those formed in overwound telephone cords) (figure 8). This behaviour could be successfully modelled using an extension of the WLC model of DNA incorporating the torsional energy termed rodlike chain, RLC [91, 92]. However, for larger forces and $|\sigma| > 0.01$ significant deviations from the theoretical predictions were observed. Later experiments [82] were able to demonstrate that, for negative supercoiling, forces beyond 0.5 pN led to local denaturation of the DNA duplex. This involved probing the stretched molecule with 1 kb segments of single-stranded DNA that were complementary to

selected regions of the tethered DNA. The hybridization of these probes with the corresponding denatured zones of the underwound and stretched target DNA led to a visible broadening of the negative branch of the extension versus σ curves. These experiments not only confirmed that denaturation was indeed taking place but also, via changes in the threshold values at which hybridization of the various probes took place ($n = -500$ for 70% AT, but $n < -3000$ for 50% AT), showed that AT-rich regions, as would be expected, were the first to denature.

The results obtained for stretched and positively supercoiled DNA were somewhat more surprising [28, 83]. Measurements carried out for values of $\sigma > 0.037$ and $F > 0.3$ pN suggested that B-DNA coexisted with a new form of highly overwound DNA with only 2.6 bp/turn and a length roughly 75% greater than that of B-DNA. Molecular modelling carried out under torsional constraints was able to propose a structure for this unusual DNA [83]. The new structure was obtained by virtually turning normal B-DNA inside out. Watson–Crick hydrogen bonding was completely disrupted and the resulting, unpaired bases were exposed on the outside of the structure, while the phosphodiester backbones were tightly packed in the middle (figure 9). Using glyoxal, a chemical which only reacts with unpaired DNA bases, it was possible to demonstrate that this structure was compatible with the state induced by combined stretching and overtwisting. This new form of DNA was named P-DNA in reference to the bases-outside model originally proposed for DNA by Pauling and Corey [93], although their model was actually a triple helix. The geometry of P-DNA, with a twist of 137° and a rise of 0.58 nm/bp, turned out to be very close to that proposed by Liu and Day [94] for the DNA of the filamentous bacteriophage pf1, although, in this case, the DNA was a single-stranded circular molecule (incapable of extensive base pairing) and the interwound structure (termed paraxial DNA by Liu and Day) is maintained not by torsional stress, but by an external protein scaffold.

The developments described here involving tethered and torsionally constrained DNA open the route for a variety of other experiments. Environmental effects on DNA supercoiling have already been studied by varying salt concentration and composition [28]. It has also been possible to look at the 'braiding' of two adjacent DNA molecules, experiments that have given rise to evidence that an electrostatic collapse supposedly leading to closely interwound duplexes [28] could take place. The most promise lies however in the study of DNA–protein interactions, where controlling extension, supercoiling and environmental factors offers many new possibilities [97] that have already begun to be exploited with a series of studies of both topoisomerases [98] and polymerases [99].

From the point of view of modelling, it has already been noted that the WLC model, originally developed by Marko and Siggia [37, 100], has been successful in reproducing the behaviour of supercoiled and stretched DNA in the regimes where alternative DNA structures do not play an important role. In this context, we can cite the extensive work of Vologodskii and Marko [101] using Monte Carlo simulations and discrete WLC representations. It is also worth noting that Nelson has shown that torsional stress can build up in DNA even without requiring tethering of the molecule. This is linked to the hydrodynamic effects of natural, anisotropic bends within DNA, which can favour crankshaft motions over the spinning of the molecule around its axis. Nelson's estimates suggest that natural DNA is effectively 'spin-locked' on a length scale corresponding to roughly 1 kb [102].

4.1.3. Strand separation. Sequencing genomes by 'unzipping' the strands of a single DNA and following the force fluctuations was considered from a theoretical point of view by Viovy *et al* in an article published in 1994 [103]. This work emphasized the difficulty of opening single pairs due to the elasticity of the single-strand segments created by the unzipping procedure. A later article by Thompson and Siggia [104] added the influence of thermal agitation, but

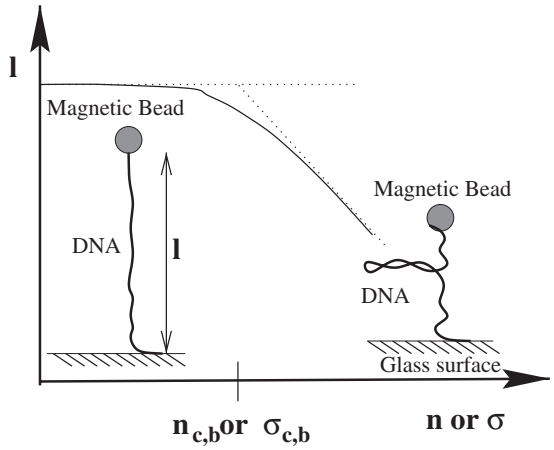

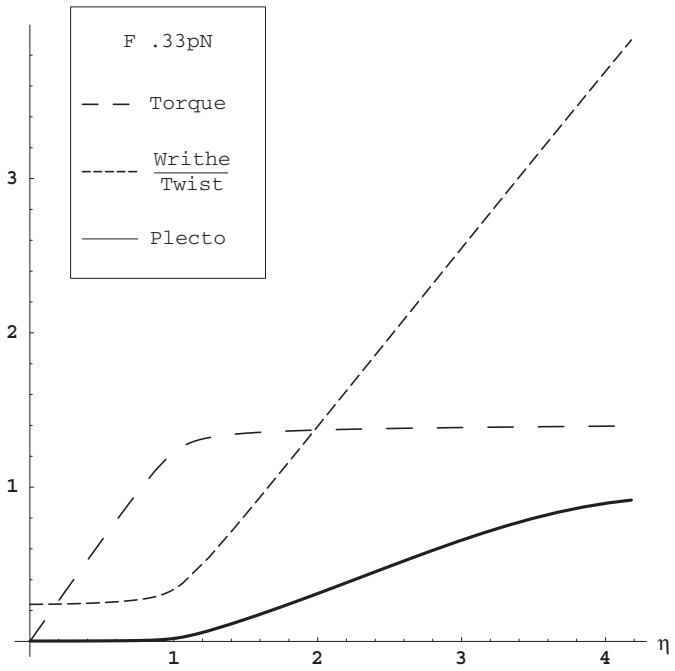

Figure 8. Top: schematic view of the buckling transition for a twisted rubber tube (dotted curve) or a DNA molecule (solid curve). Below a critical number of turns ($n_{c,b}$) the rubber tube's torque increases linearly as it stores twisting energy. When ($n_{c,b}$) turns have been added the system abruptly exchanges twisting energy for bending energy and plectonemes begin to form. The plectonemes grow linearly with subsequent twisting and the torque remains constant thereafter. In the case of DNA the same picture holds, except for the fact that thermal fluctuation rounds off the transition, which takes place at $n_{c,b}$. Bottom: results from the RLC model corresponding to a stretching force of $F = 0.33$ pN. The x-axis represents the supercoiling variable $\eta = 2\pi n \xi_T / l_0 \simeq 95\sigma$ [91], and the y-axis is in arbitrary units. The long-dashed curve represents the torque acting on the DNA: as described above, it increases linearly until $\eta_{c,b} \sim 1\ \sigma \sim 0.01$) and remains essentially constant thereafter. The short-dashed curve represents the ratio of writhe to twist: note that the writhe is never zero and increases rapidly as $\eta > 1$. Finally, the full curve measures the fraction of plectonemes in DNA: stable supercoiled structures only appear after the torsional buckling transition has been passed.

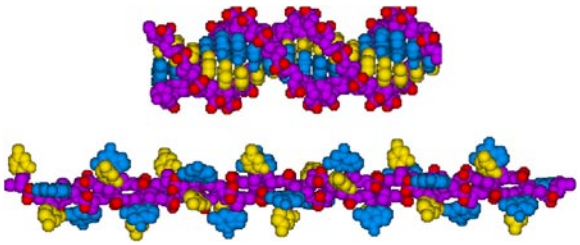

Figure 9. Structure of P-DNA deduced from molecular modelling. Space filling models of a $(dG)_{18}(dC)_{18}$ fragment in B-DNA (top) and P-DNA (bottom) conformations. The backbones are coloured purple and the bases blue (guanine) and yellow (cytosine). The anionic oxygens of the phosphate groups are shown in red. These models were created with the JUMNA program [95, 96], by imposing twisting constraints on helically symmetric DNA with regularly repeating base sequences.

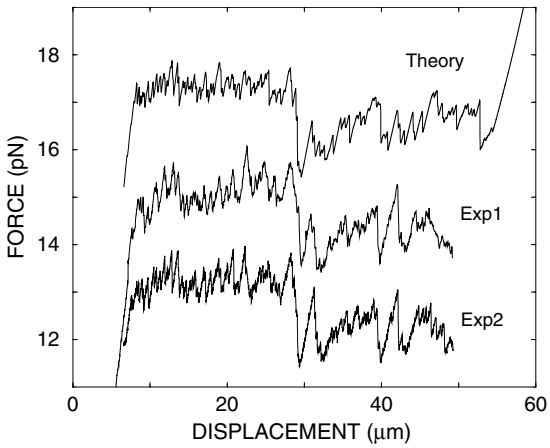

Figure 10. Force curves for opening the λ phage DNA obtained by Heslot's group. The three curves have been shifted by 2 and 4 pN for clarity. The two experimental curves have been obtained at different unzipping velocity 40 nm s^{-1} (EXP2), 200 nm s^{-1} (EXP1). The theoretical curve is derived from the GC content of the molecule. (This curve has been extracted from [12].)

neither of these models took into account the impact of a variable base sequence. When the corresponding experiment was carried out in 1997 by the Heslot group [11, 12], DNA turned out to open via a stick–slip mechanism, with periods of only slight extension, coupled to increasing molecular strain, interrupted by the sudden opening of segments containing tens to hundreds of base pairs. These experiments were performed using a DNA construct consisting of two λ DNA molecules attached together, and capped at one end by oligomeric segments. One of these molecules served as a double-stranded linker and was attached to a glass slip using a DIG–antiDIG junction, while a dangling strand between the two molecules was attached to a paramagnetic bead via a biotin–streptavidin junction (figure 3). This bead was placed in contact with a glass microneedle, while the glass slip could be accurately translated using a piezoelectric stage. This construction allowed the two strands of the second λ DNA molecule to be separated, following the force fluctuations via the deflections of the glass microneedle (which had previously been calibrated).

The results of this experiment showed that the DNA strands could be separated with an average force of 13 pN. Force fluctuations were of the order of 2 pN. These fluctuations,

although small, were well above the sensitivity of the experiment (roughly 0.2 pN) and were reproducible when the strand separation was repeated for a single molecular construct. The saw-tooth profiles along the force curve correlated with fluctuations in the local GC content of the λ DNA molecule (figure 10). This correlation was confirmed in an elegant manner by reversing the sense of the opening λ DNA in the molecular construct. Although the slow force rise of the saw-tooth profiles was now reversed, the rapid force drop, corresponding to opening a base pair segment, correlated well with that from the original experiment. In contrast to protein unfolding experiments (see section 4.3), varying the opening rate from 20 to 800 nm s^{-1} did not significantly change the recorded force profile [105]. This difference is related to the much lower energy barriers associated with base pair opening compared with the unfolding of protein domains. This enables the opening DNA molecule to remain in thermal equilibrium throughout the experiment and implies that the corresponding force variations reflect free-energy changes for the loss of base pairing and stacking. If we assume that each base pair disruption corresponds to liberating roughly 1.2 nm of single-stranded DNA (i.e. 0.6 nm for each phosphodiester backbone), then a 13 pN force corresponds to an average energy per base pair of 2.2 kcal mol^{-1}. This is of the order of the estimated free energy changes for denaturing a single base pair within a DNA oligomer [106].

Sequence effects have now been incorporated in equilibrium statistical mechanics models of strand separation, both by the authors of the experimental study [12, 105] and by other groups [107]. Molecular modelling of the strand separation experiment for a DNA oligomer has also been carried out, leading to force fluctuations which again reflect the base sequence and also show that weaker AT pairs can break almost simultaneously as the length separating the ends of the oligomer is monotonically increased [80]. However, this modelling involves enthalpy calculations without thermal fluctuations rather than free-energy calculations. In consequence, the mean force necessary to separate the two stands was much higher (∼70 pN). This implies an average enthalpy change of 12 kcal mol^{-1}/bp disruption, which is similar to values deduced from (nonequilibrium) AFM experiments involving strand separation for DNA oligomers (see [4, 6] section 4.1.1) and to estimated melting enthalpies based on experimental studies [106].

4.2. RNA

The first, and, until now, only mechanical study of RNA [5], has investigated the influence of loading rate on unfolding and refolding of three different variants of the P5abc ribosomal domain: a simple RNA hairpin (termed P5ab), the same hairpin containing an additional helix and, therefore, a three-helix junction (P5abΔA) and, finally, the complete P5abc domain, which contains an A-rich bulge and is packed into a stable tertiary structure in the presence of Mg^{2+}.

Both ends of these RNA molecules were bound to polystyrene beads via RNA/DNA hybrid segments. One of the beads was then held in an optical trap, while the other bead was linked to a piezo-electric actuator via a micropipette. As the simple RNA hairpin was extended, the authors observed an increase of the force until a plateau was reached at 14.5 pN, close to the value obtained for the DNA unzipping [11, 12]. The transition from the folded to the unfolded state was reversible in less than 10 ms, indicating a thermal equilibrium at the critical force. By using a feedback mechanism to fix the force close to the plateau value, it was possible to shift the folded–unfolded equilibrium and to control the kinetics and thermodynamics of the folding process. The presence of an additional helix and of the three-helix junctions in P5abcΔA slows down the folding–unfolding process, presumably because of the necessity of nucleating two separate hairpins. The mechanical unfolding of the complete RNA domain

also corresponds to a two-step process with distinct kinetic barriers in the presence of Mg^{2+}. Without Mg^{2+}, the barriers are removed and the unfolding–folding process becomes reversible. Comparison with the unfolding of the partial domains suggests that the unfolding occurs by the opening of the P5a helix and then propagates to the rest of the molecule.

4.3. Proteins

Protein function is acquired through specific folding. Until recently the stability of folded proteins has been studied mainly by chemical and thermal denaturation. However, certain proteins such as the muscle proteins (titins), extracellular matrix proteins (tenascin) or cytoskeletal proteins (spectrin) are specifically designed to withstand forces in addition to chemical changes in their environment. Recent developments in single-molecule manipulation techniques (AFM, SFM, ...) have thus been applied to studying the mechanical properties of such proteins and to induce their unfolding via mechanical forces [33, 108–115]. These techniques have also demonstrated their power for studying the anchoring forces of the membrane proteins, such as bacteriorhodopsin, within phospholipid bilayers, as well as inducing unfolding by extraction of the protein from the bilayer [116].

A common feature of the muscle and skeletal families of proteins is that they exist as giant polymers, including multiple, individually folded protein domains. Thus, titin is composed of roughly 300 successive immunoglobulin (Ig) and fibronectin (FN3) domains and unique PEVK (70% proline, glutamic acid, valine and lysine residues) regions. The Ig and FN3 domains are localized in the so-called A-band of the molecule and the PEVK region is located in the I-band, while the Ig domains are distributed throughout the molecule [117]. The Ig and FN3 domains are both β-sandwich conformations, while the PEVK region is unstructured. Tenascin is made up of successive subunits including mainly tandem FN3 domains [118], while spectrin is composed of subunits made of three antiparallel α-helices connected by a helical linker [119].

In their relaxed state these proteins form coiled structures, maximizing the entropy of their segments. Linearization of the protein polymer only requires weak forces to overcome this entropic elasticity. Once the polymer approaches its full contour length, its resistance rises considerably. AFM studies of such pulling display a characteristic saw-tooth pattern for the force versus extension curves [33, 111–113, 115, 120, 121]. The form of these curves can be explained by a simple model: a domain of the protein, which is covalently attached to the surface, is picked up by absorption on the AFM tip. As the tip is retracted, the domain is stretched and strain builds up until a critical force is reached. At this force, the domain unfolds and the corresponding increase in length releases the accumulated strain. The number of saw-tooth patterns then corresponds to the number of unfolded domains and the amplitude reflects the mechanical stability of the folded domain (figure 11). In addition, the spacing between the peaks reflects the number of amino acids that each unfolding event adds to the total length of the polymer. Domains of equal size should therefore yield evenly space peaks.

Unfortunately, the heterogeneity of native proteins complicates the interpretation of the AFM studies. A modular protein, such as titin, contains multiple copies of several different domains which are susceptible to unfolding and it is difficult to relate individual unfolding peaks in the force–extension curve to any specific domains. This problem can be overcome using molecular biology techniques which make it possible to construct polyproteins consisting of multiple copies of a unique protein fold.

Using this approach, saw-tooth extension curves were obtained for pure Ig domains [33] and, later, for pure FN3 domains [111]. The mean force at which the FN3 domain unfolds is 137 pN and the mean interval between the saw-tooth peaks is roughly 25 nm [110, 111].

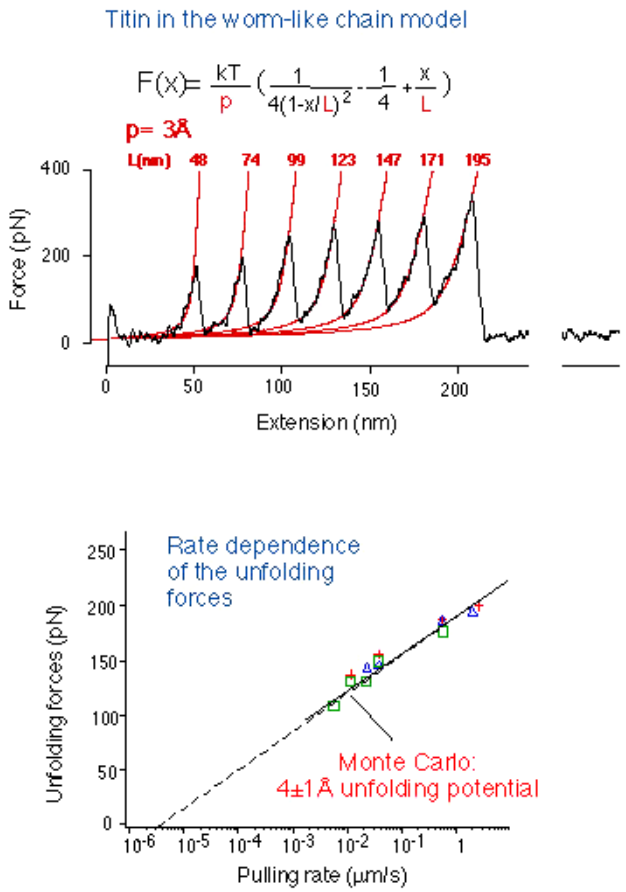

Figure 11. Force–extension curve obtained by pulling on titin protein. The saw-tooth behaviour corresponds to the unfolding of the different domains of the protein. The experimental data are compared with a numerical model using the WLC model and a two-level model. The bottom curve indicates that the unfolding force increases as the pulling rate is increased. (This image has been taken from the web site of Rief and Gaub: http://www.biophysik.physik.uni-muenchen.de)

The study of the Ig domains leads to more complex results. The force–extension curves for a fragment of titin consisting of domains I27–I34 revealed up to eight unfolding peaks at forces ranging from 150 to 300 pN and an increase of the contour length of 26.6 nm (89 amino-acid residues) [33, 111]. The height of the peaks increases with each unfolding event, suggesting that different domains have different mechanical instabilities. Furthermore, recent AFM experiments [115] suggest the presence of an unfolding intermediate in both the I27 and I28 modules. This is deduced from a small shoulder in the curve corresponding to a force-induced transition that elongates the molecule by only 0.66 nm at forces of 100 pN and 150 pN for I27 and I28 respectively. After this transition, the force increases again to a maximum of about 200–300 pN, where domain unfolding occurs, with a total extension of 28 nm. This small extension is most prominent in the first unfolding peak and then decreases with each peak until it finally disappears [115].

Modelling studies using steered molecular dynamics (SMD) [54, 55, 122] have been very useful in understanding the Ig unfolding pathway at the atomic scale. The Ig domain is

composed of two β-sheets that are held together by hydrogen bonds and hydrophobic core interactions. One sheet is composed of the A, B, D and E β-strands and the other is formed by the A′, C, F and G β-strands. The structure is locked by six to eight hydrogen bonds between the C- and the N-terminal β-strands (see [123], respectively G and A–A′, parallel to each other and pointing in opposite directions). SMD used to induce forced unfolding of I27 [54, 55, 122] suggests that when a force is applied to the C- and N-terminal strands the first event is the breaking of the two hydrogen bonds between the A and B β-strands, while the greatest resistance to unfolding comes from the hydrogen bonds between the A′ and G β-strands. This burst event leads to an unfolding intermediate and, depending on how the forces are applied, results in an extension of 0.6–1.2 nm. This predicted value correlates well with the small transition extension of 0.66 nm observed experimentally. After this bond breaking, the remainder of the domain is principally held by hydrophobic interactions and can unravel with little resistance.

SMD simulations of other proteins, and particularly of FN3 domains [55, 114], has been helpful in understanding the difference in the experimentally observed forces necessary to mechanically unfold proteins [111, 124]. The FN3 domain, like the Ig domain, is constituted of a β-sandwich with its N- and C-terminal strands arranged in an anti-parallel fashion. However, in the case of FN3 the N- and C-termini are not directly bound to each other, but rather interact with nonterminal strands. SMD simulations show a greater degree of deformation of the domain upon stretching and a more gradual breaking of hydrogen bonds that initiates the unfolding. This smoother pathway for the FN3 domain explains the experimental observation that the forces needed to unravel FN3 are roughly 20% weaker than those necessary for the Ig domain [111].

A first AFM study of spectrin unfolding showed that its domains unravel at much lower forces (25–35 pN) than those of either titin or tenascin. Spectrin unfolds in a cooperative manner and no intermediate was observed [120]. However, a more recent study, using engineered protein constructs with 16 spectrin domains, reveals the existence of at least one intermediate [121]. A partial unfolding event is detected at a force of 60 pN with an extension of 15.5 ± 3.5 nm, followed by a second and more significant unfolding at 80 pN with an extension of 31 ± 7 nm. The difference in unfolding forces between titin Ig and spectrin-like repeats by a factor of up to five is dramatic. This difference reflects the fact that the tertiary structure of an α-helix bundle is maintained by hydrophobic forces and is thus mechanically less stable than multiply hydrogen-bonded β-sheet folds. The unfolding pathway is unknown for α-spectrin, but SMD simulations of a typical α-helical domain belonging to the electron transport protein cytochrome c6 (cc6, a five-helix protein) have been made [55]. The results show an extension of the α-helices near the N- and C-termini in the first stages of unfolding, followed by the separation of the helices and the destruction of their hydrophobic interactions. The forces needed to unravel the cc6 domain are much weaker than those observed during the simulations of the Ig and FN3 domains [55]. These simulations show no intermediate force peaks, but rather a smooth and continuous unfolding process. Similar results have been obtained using molecular mechanics modelling studies of the unfolding of secondary structure protein elements [51]. The α-helix extension force shows a smooth transition from (i)–$(i+4)$ hydrogen bonds to a more extended (so-called 3_{10} conformation) with (i)–$(i+3)$ bonds, before the complete loss of the hydrogen bonds at higher forces. These authors also studied the lateral separation of α-helices, which is dominated by local van der Waals contacts and required relatively low forces.

We lastly turn to the field of integral membrane proteins. By combining AFM and single-molecule force spectroscopy, it has been possible to study the unfolding of the α-helical membrane protein bacteriorhodopsin [116]. Bacteriorhodopsin is composed of

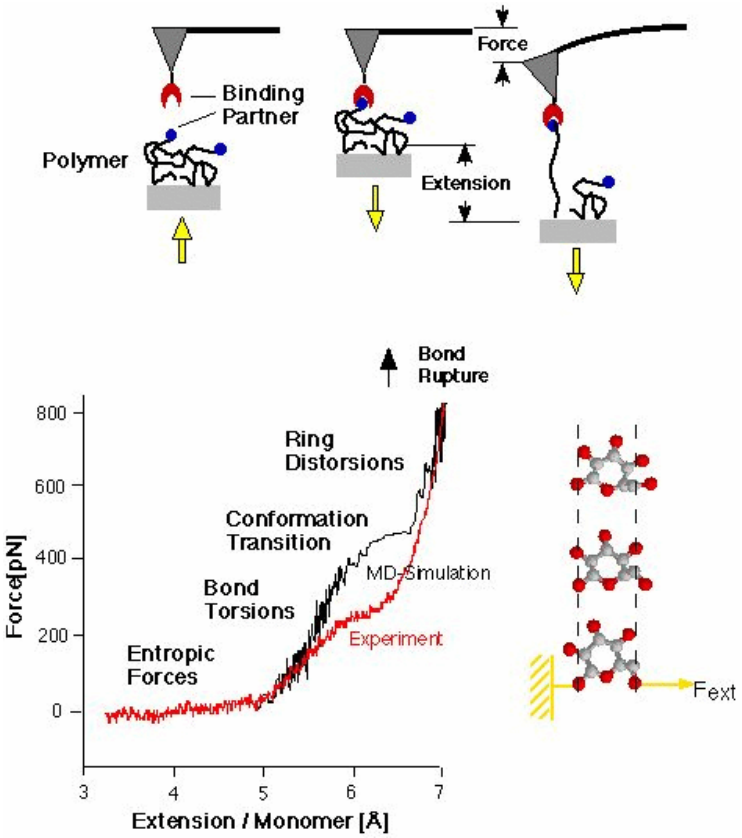

Figure 12. Measurement principle and results on the stretching of a dextran polymer. The force versus extension curve of dextran displays a plateau around 250 pN, corresponding to a sugar conformational change. The results of a numerical simulation performed at higher loading rates (black) predict a transition at a higher pulling force. (Image taken from the web page of Rief and Gaub: http://www.biophysik.physik.uni-muenchen.de)

seven transmembrane helices, labelled A–G, connected by extra-membrane loops [125]. Single-molecule experiments were performed by localizing and then pulling individual bacteriorhodopsin out of the membrane. The resulting vacancies are imaged by AFM, to ensure full protein extraction had occurred. Anchoring forces of between 100 and 200 pN were found for the different transmembrane helices. The force–extension curves notably show a pairwise extraction for helices G–F and E–D, while helices B and C unfold one after the other. Experiments with a cleaved E–F loop shift the extension curve, indicating a pairwise extraction of E–D helices, but a different unfolding behaviour for helices B and C. This is interpreted as stabilization of the later helices by G and F, which are not extracted in the cleaved protein. This study is an elegant demonstration of how force-induced structural changes combined with high-resolution imaging can be a powerful approach for determining not only a detailed map of a protein unfolding pathway, but also the local interactions within the membrane.

4.4. Polysaccharides

Polysaccharides constitute a very large family of linear and branched polymers based on the pyranose rings and varying in both the sugar monomers they contain and the position and orientation of the glycosidic bonds (equatorial or axial) which link successive sugar rings. Biologically important polysaccharides occur in a wide variety of cellular structures and also play critical roles in cell adhesion. They are often subjected to considerable tensile stress and are thought to respond to this stress by elastic deformation. AFM has therefore been used to characterize the elasticity of single polysaccharide molecules [126–130].

Ab initio calculations suggested that polysaccharides whose glycosidic linkages are attached equatorially to the pyranose ring will display no force-induced transition. In contrast, polysaccharides with axial linkages could show abrupt force-induced transitions (from so-called chair to boat conformers with an eventual transition to an inverted chair), leading to an increased distance between the glycosidic bonds under the transitions [128, 130]. To test this hypothesis, AFM experiments were carried out on different polysaccharides having up to two axial linkages (figure 12). Cellulose, which has only equatorial linkages, effectively obeys the FJC model of polymer elasticity, and shows no structural transitions [127, 130]. In contrast, other polysaccharides with one or two axial linkages show respectively one or two abrupt force-induced length transitions [126, 128–130]. These transitions are reversible and the force–extension curves show no hysteresis. They consequently do not involve pyranose ring cleavage and apparently confirm the existence of transitions due to changes in the pyranose conformers. This result is important for understanding polysaccharide elasticity, particularly because it is incompatible with the classical view that pyranose sugar rings are conformationally rigid.

4.5. Macromolecule–ligand complexes

In their pioneering AFM experiments, Florin *et al* [13] used applied forces to probe avidin–biotin interactions. Avidin was bound to the biotinylated tip of an AFM cantilever and brought into contact with biotinylated beads that had most of their binding sites blocked to prevent multiple ligand binding with the tip. Avidin has two pairs of biotin-binding sites, one pair in contact with the tip and the other (on the opposite side of the molecule) in contact with the bead. Upon retraction of the AFM tip, the cantilever bent (due to the adhesion of avidin with the biotin on the bead) and then gave way in a series of small jumps. A statistical analysis of the jumps revealed that the measured adhesion forces were multiples of an elementary force quantum of 160 ± 20 pN. This force quantum was attributed to the interaction of a single biotin–avidin pair. Similar experiments were also carried out with complexes of avidin or streptavidin with biotin analogues. A direct comparison between the thermodynamic parameters of five different avidin–biotin pairs and the unbinding forces allowed the authors to demonstrate a direct proportionality between enthalpy changes during complex formation and unbinding forces. These experiments suggested a two-step process of dissociation with initial enthalpy changes being followed by entropic changes as the departing ligand becomes more mobile.

One year before these early AFM experiments, a simulation of streptavidin with biotin (or biotin analogue) binding was carried out using MD simulations in combination with free-energy perturbation techniques [131]. These calculations were of considerable help in deconvoluting the various contributions to protein–ligand recognition. However, because this approach uses a nonphysical pathway to compute the free-energy difference between bound and unbound states, it was impossible to derive the rupture force obtained from the AFM experiments. This drawback was overcome in the work of Grubmüller *et al* [52] and Izrailev *et al* [53]. Both

these studies used the known crystallographic structure of streptavidin–biotin and avidin–biotin complexes as input. Biotin was then extracted from the protein binding pocket by pulling on the distal end of the ligand with a pseudo-mechanical spring, the centre of mass of the protein being fixed. It should be noted that the binding pockets of avidin and streptavidin have a very similar structure but avidin forms an additional nonpolar interaction and three additional hydrogen bonds with biotin. Moreover, the flexible loop which closes the binding pocket in avidin is longer and closes more tightly behind biotin in the bound state. The MD simulations led to a complex set of molecular interactions along the unbinding trajectories. During the initial displacement ($<$0.2 nm) unbinding began with the detachment of the biotin head group (a ureido ring) from a matrix of hydrogen bonds, water bridges and nonpolar interactions deep inside the binding pocket. Next, forces reach maximal values followed by sudden displacements of the ligand. This occurred at a distance of $\sim$0.5 nm in the biotin–streptavidin simulation and was attributed to rupture of a transient network of water bridges and hydrogen bonds. For the biotin–avidin simulation, the displacement occurred at $\sim$0.4 nm due to the rupture of both polar and nonpolar bonds. Beyond this point, biotin continues to form transient interactions with peripheral polar groups of the binding site until a displacement of $\sim$1.4 nm.

Comparison of the MD simulations and the AFM experiments showed quite good agreement with the streptavidin–biotin simulation, but for the avidin–biotin study the simulated forces were too strong by several orders of magnitude. It should be added that, despite the good comparison in the case of the streptavidin–biotin simulation, only one streptavidin monomer was included in this simulation instead of the two needed to form the complete biotin-binding pocket seen in the crystallographic structure. This would be expected to weaken the ligand–protein interaction. The underlying problem, as pointed out by Izrailev *et al* [53], is the different timescales of the simulation and the experiment. During AFM experiments the observation period ($\sim$1 ms) is long enough to allow the ligand to thermally equilibrate, spontaneously overcoming potential barriers. On the other hand, the unbinding induced by MD simulation occurs on a very short timescale ($\sim$1 ns) in a dissipative regime where irreversible work is being generated. Such simulations pass over energy barriers and actually measure frictional forces. Consequently, the unbinding event observed during the simulation cannot be extrapolated to the experimentally observed rupture. Balsera *et al* [132] used a one-dimensional stochastic model to evaluate the contribution of dissipation forces in order to relate the rupture forces observed in MD simulations with the dissociation induced in AFM experiments. The effect of dissipation is represented by the friction coefficient γ, that can be obtained by MD simulation, and is related to the magnitude of the random forces that perturb the ligand. Once γ is known it can be used to estimate the amount of irreversible work produced during forced unbinding. The reader is also referred to the work of Hummer *et al* [59], where the identity between thermodynamic free-energy differences and irreversible work is used to extract equilibrium properties from both pulling experiments and simulation.

Many experimental studies have demonstrated that the force at which an interaction will break depends on the rate at which the force is applied. The ligand within a macromolecule–ligand complex is involved in many interactions with residues in the binding pocket and these interactions have to be overcome during dissociation. These interactions simply represent barriers within the energy landscape. Evans and Ritchie [58] showed that a relationship exists between the width of the distribution of forces needed for the dissociation and the energy landscape under investigation. This study is based on Kramers' theoretical work, showing that the maximum of the distribution of forces (termed the most probable rupture force) is related to the logarithm of the loading rate. The plot of the force against the logarithm of the loading rate shows distinct linear regimes, each being interpreted as linked to a specific barrier. The development of a new experimental method, termed

dynamic force spectroscopy (DFS), allowed Merkel *et al* [133] to study the unbinding forces of the streptavidin–biotin system over a wide range of loading rates from 0.05 to 60 000 pN s^{-1}. In this way, the authors obtained rupture forces ranging from 5 to 170 pN as a function of the loading rate. They were then able to compare the activation barriers derived from their spectra with the shape of the energy landscape derived from simulations (based on the instantaneous biotin–avidin interaction energies extracted from the simulation of Israilev *et al* [53]). They obtained good correlation in both high- and intermediate-binding regimes, where the transition states persist over the corresponding range of loading rates. However, the barrier found from the low-binding regime, attributed in the MD simulation to the flexible loop closing the pocket, appears at different places when comparing simulation and experimental results. In a complementary study, Galligan *et al* [60] adopted a combination of traditional reaction coordinate mapping and Brownian dynamics to predict the dynamic force spectrum for streptavidin–biotin dissociation. They simulated the rupture force over a wide range of loading rates (beyond those possible for all-atom simulations) and found good agreement with the experimental work of Merkel *et al* [133].

Another ligand–protein system which has been studied is the antigen–antibody pair formed by fluorescein and antifluorescein antibodies. The results obtained in this case are quite different from those cited above. Nine mutants of three antifluorescein antibodies have been studied at different loading rates [134]. The authors demonstrated that (i) there is a linearity of the unbinding force measured versus the loading rate, implying only one transition state, and (ii) the measured unbinding forces for the nine antibody mutants correlated well with the dissociation rate measured in solution, indicating that the same transition state must be crossed in spontaneous and forced unbinding and that the unbinding path under load must be close to the spontaneous path. These differences show the sensitivity of such systems to the structure of the binding pocket and to the exact nature of the binding interactions.

5. Conclusions

In less than a decade, the development of single-molecule approaches has opened up a new chapter in the study of biological macromolecules. The results obtained have been interesting not only from the point of view of statistical physics, but also from a biological standpoint. Most importantly, they have emphasized the role played by forces within biological systems and, with the help of molecular modelling, have begun to explain how nucleic acids, proteins, polysaccharides and macromolecule–ligand complexes will react to imposed forces. Much still remains to be done in this field, notably via the extension of single-molecule techniques to studies of the macromolecular complexes (protein–DNA, protein–RNA, protein–protein) which are fundamental to understanding integrated biological functions and underlie such important processes as DNA translation and replication, protein synthesis and cellular transport. Such studies will profit from coupling to optical experiments (notably using fluorescence energy transfer, evanescent wave, two-photon and confocal techniques) and to increasingly refined molecular simulations. The results will undoubtedly yield new insights into structural, energetic and kinetic aspects of the functioning of a wide variety of biological machines.

Acknowledgments

The authors wish to thank U Bockelmann and F Heslot for providing figure 10, F Pincet and E Perez, who gave the BFP illustration in figure 3, and H Gaub for figures 11 and 12. We

thank C Bustamante, D Chatenay, H Clausen-Schaumann, H Gaub, J-F Léger and S Smith for sharing their data shown in figure 6. We also thank the CNRS, École Normale Supérieure, Paris 6 and 7 Universities for their support. JFA, DB and VC also wish to thank ARC (Association pour la Recherche sur le Cancer) for their funding.

References

[1] Strick T, Allemand J F, Bensimon D, Bensimon A and Croquette V 1996 The elasticity of a single supercoiled DNA molecule *Science* **271** 1835 –7
[2] Cluzel P, Lebrun A, Heller C, Lavery R, Viovy J-L, Chatenay D and Caron F 1996 DNA: an extensible molecule *Science* **271** 792–4
[3] Smith S B, Finzi L and Bustamante C 1992 Direct mechanical measurements of the elasticity of single DNA molecules by using magnetic beads *Science* **258** 1122–6
[4] Noy A, Vezenov D V, Kayyem J F, Meade T J and Lieber C M 1997 Stretching and breaking duplex DNA by chemical force microscopy *Chem. Biol.* **4** 519–27
[5] Liphardt J, Onoa B, Smith S B, Tinoco I Jr and Bustamante C 2001 Reversible unfolding of single RNA molecules by mechanical force *Science* **292** 733–7
[6] Rief M, Clausen–Schaumann H and Gaub H E 1999 Sequence-dependent mechanics of single DNA molecules *Natl Struct. Biol.* **6** 346–9
[7] Allemand J-F, Bensimon D, Jullien L, Bensimon A and Croquette V 1997 pH-dependent specific binding and combing of DNA *Biophys. J.* **73** 2064–70
[8] Shivashankar G V, Feingold M, Kritchevsky O and Libchaber A 1999 RecA polymerization on double-stranded DNA by using single-molecule manipulation: the role of ATP hydrolysis *Proc. Natl Acad. Sci. USA* **96** 7916–21
[9] de Gennes P G 1979 *Scaling Concepts in Polymer Physics* (Ithaca, NY: Cornell University Press)
[10] Finer J T, Simmons R M and Spudich J A 1994 Single myosin molecule mechanics: piconewton forces and nanometre steps *Nature* **368** 113–9
[11] Essevaz-Roulet B, Bockelmann U and Heslot F 1997 Mechanical separation of the complementary strands of DNA *Proc. Natl Acad. Sci. USA* **94** 11 935–40
[12] Bockelmann U, Essevaz-Roulet B and Heslot F 1997 Molecular stick–slip revealed by opening DNA with piconewton force *Phys. Rev. Lett.* **79** 4489–92
[13] Florin E L, Moy V T and Gaub H E 1994 Adhesion force between individual ligand–receptor pairs *Science* **264** 415–7
[14] Moy V T, Florin E-L and Gaub H E 1994 Intermolecular forces and energies between ligands and receptors *Science* **266** 257–9
[15] Williams J M, Hon T and Beebe T P Jr 1996 Determination of single-bond forces from contact force variances in atomic force microscopy *Langmuir* **12** 1291–5
[16] Dammer U, Popescu O, Wagner P, Anselmetti D, Günherodt H-J and Misevic G N 1995 Binding strength between cell adhesion proteoglycans measured by atomic force microscopy *Science* **267** 1173–5
[17] Lee G U, Chrisey L A and Colton R J 1994 Direct measurement of the forces between complementary strands of DNA *Science* **266** 771–3
[18] Smith S B, Cui Y and Bustamante C 1996 Overstretching B-DNA: the elastic response of individual double-stranded and single-stranded DNA molecules *Science* **271** 795–9
[19] Lebrun A and Lavery R 1996 Modelling extreme deformations of DNA *Nucl. Acids Res.* **24** 2260–7
[20] Ishijima A, Doi T, Sakurada K and Yanagida T 1991 Sub-piconewtown force fluctuations of actomyosin in vitro *Nature* **352** 301–6
[21] Simmons R M, Finer J T, Chu S and Spudich J A 1996 Quantitative measurements of force and displacement using an optical trap *Biophys. J.* **70** 1813–22
[22] Amblard F, Yurke B, Pargellis A and Leibler S 1996 A magnetic manipulator for studying local rheology and micromechanical properties of biological system *Rev. Sci. Instrum.* **67** 1–10
[23] Gosse C and Croquette V 1999 Magnetic tweezers *Rev. Sci. Instrum.* in preparation
[24] Evans E, Ritchie K and Merkel R 1995 Sensitive force technique to probe molecular adhesion and structural linkages at biological interfaces *Biophys. J.* **68** 2580–7
[25] Smith S B 1998 Stretch transitions observed in single biopolymer molecules (DNA or protein) using laser tweezers *Thesis* University of Twente
[26] Einstein A 1956 *Investigation of the Brownian Theory of Movement* (New York: Dover)
[27] Reif F 1965 *Fundamentals of Statistical and Thermal Physics* (New York: McGraw-Hill)

[28] Strick T, Allemand J-F, Bensimon D and Croquette V 1998 The behaviour of supercoiled DNA *Biophys. J.* **74** 2016–28
[29] Kishino A and Yanagida T 1988 Force measurement by micromanipulation of a single actin by glass needles *Nature* **334** 74–6
[30] Ishijima A, Kojima H, Funatsu T, Tokunaga M, Higuchi H, Tanaka H and Yanagida T 1998 Simultaneous observation of individual ATPase and mechanical events by a single myosin molecule during interaction with actin *Cell* **92** 161–71
[31] Leger J-F 1999 L'ADN: une flexibilité structurale adaptée aux interactions avec les autres macromolécules de son environnement *PhD Thesis* Université Louis Pasteur Strasbourg I
[32] Dammer U, Hegner M, Anselmetti D, Wagner P, Dreier M, Huber W and Guntherodt H-J 1996 Specific antigen/antibody interactions measured by force microscopy *Biophys. J.* **70** 2437–41
[33] Rief M, Gautel M, Oesterhelt F, Fernandez J M and Gaub H E 1997 Reversible unfolding of individual titin immunoglobulin domains by AFM *Science* **276** 1109–12
[34] Léger J F, Robert J, Bourdieu L, Chatenay D and Marko J F 1998 RecA binding to a single double-stranded DNA molecule: a possible role of DNA conformational fluctuations *Proc. Natl Acad. Sci. USA* **95** 12 295–6
[35] Yin H, Wang M D, Svoboda K, Landick R, Block S and Gelles J 1995 Transcription against a applied force *Science* **270** 1653–7
[36] Bustamante C, Marko J F, Siggia E D and Smith S 1994 Entropic elasticity of λ-phage DNA *Science* **265** 1599–600
[37] Marko J F and Siggia E D 1994 Fluctuations and supercoiling of DNA *Science* **265** 506–8
[38] Vologodskii A V 1994 DNA extension under the action of an external force *Macromolecules* **27** 5623–5
[39] Bouchiat C, Wang M D, Block S M, Allemand J-F, Strick T R and Croquette V 1999 Estimating the persistence length of a worm-like chain molecule from force–extension measurements *Biophys. J.* **76** 409–13
[40] Wang M D, Yin H, Landick R, Gelles J and Block S 1997 Stretching DNA with optical tweezers *Biophys. J.* **72** 1335–46
[41] Baumann C, Smith S, Bloomfield V and Bustamante C 1997 Ionic effects on the elasticity of single DNA molecules *Proc. Natl Acad. Sci. USA* **94** 6185–90
[42] Hogan M E and Austin R H 1987 Importance of DNA stiffness in protein–DNA binding specificity *Nature* **329** 263–6
[43] Sagui C and Darden T A 1999 Molecular dynamics simulations of biomolecules: long-range electrostatic effects *Annu. Rev. Biophys. Biomol. Struct.* **28** 155–79
[44] Cheatham T E, Cieplak P and Kollman P A 1999 A modified version of the Cornell *et al* force field with improved sugar pucker phases and helical repeats *J. Biomol. Struct. Dyn.* **16** 845–62
[45] Foloppe N and MacKerell A D Jr 2000 All-atom empirical force field for nucleic acids: I. Parameter optimization based on small molecule and condensed phase macromolecular target data *J. Comput. Chem.* **21** 86–104
[46] Scott W R P, Hunenberger P H, Tironi I G, Mark A E, Billeter S R, Fennen J, Torda A E, Huber T, Kruger P and van Gunsteren W F 1999 The GROMOS biomolecular simulation program package *J. Phys. Chem.* **103** 304
[47] Schaefer M, Bartels C and Karplus M 1998 Solution conformations and thermodynamics of structured peptides: molecular dynamics with an implicit solvation model *J. Mol. Biol.* **284** 835–48
[48] Tsui V and Case D 2000 Molecular dynamics simulations of nucleic acids with a generalized Born solvation model *J. Am. Chem. Soc.* **122** 2489–98
[49] Lafontaine I and Lavery R 1999 Collective variable modelling of nucleic acids *Curr. Opin. Struct. Biol.* **9** 170–6
[50] Kosikov K M, Gorin A A, Zhurkin V B and Olson W K 1999 DNA stretching and compression: large-scale simulations of double helical structures *J. Mol. Biol.* **289** 1301–26
[51] Rohs R, Etchebest C and Lavery R 1999 Unraveling proteins: a molecular mechanics study *Biophys. J.* 2760–8
[52] Grubmüller H, Heymann B and Tavan P 1996 Ligand binding: molecular mechanics calculation of the streptavidin–biotin rupture force *Science* **271** 997–9
[53] Izrailev S, Stepaniants S, Balsera M, Oono Y and Schulten K 1997 Molecular dynamics study of unbinding of the avidin–biotin complex *Biophys. J.* **72** 1568–81
[54] Lu H, Isralewitz B, Krammer A, Vogel V and Schulten K 1998 Unfolding of titin immunoglobin domains by steered molecular dynamics simulation *Biophys. J.* **75** 662–71
[55] Lu H and Schulten K 1999 Steered molecular dynamics simulations of force-induced protein domain unfolding *Proteins* **35** 453–63
[56] Krammer A, Lui H, Isralewitz B, Schulten K and Vogel V 1999 Forced unfolding of the fibronectin type III module reveals a tensile molecular recognition switch *Biophys. J.* **96** 1351–6
[57] Paci E and Karplus M 2000 Unfolding proteins by external forces and temperature: the importance of topology and energetics *Proc. Natl Acad. Sci. USA* **97** 6521–6
[58] Evans E and Ritchie K 1997 Dynamic strength of molecular adhesion bonds *Biophys. J.* **72** 1541–55

[59] Hummer G and Szabo A 2001 Free energy reconstruction from non-equilibrium single-molecule pulling experiments *Proc. Natl Acad. Sci. USA* **98** 3658–61
[60] Galligan E, Roberts C J, Davies M C, Tendler S J B and Williams P M 2001 Simulating the dynamic strength of molecular interactions *J. Chem. Phys.* **114** 3208–14
[61] MacKerell A D and Lee G U 1999 Structure, force, and energy of a double-stranded DNA oligonucleotide under tensile loads *Eur. Biophys. J.* **28** 415–26
[62] Chong L T, Duan Y, Wang L, Massova I and Kollman P A 1999 Molecular dynamics and free-energy calculations applied to affinity maturation in antibody 48G7 *Proc. Natl Acad. Sci. USA* **96** 14 330–5
[63] Wang W and Kollman P A 2000 Free energy calculations on dimer stability of the HIV protease using molecular dynamics and a continuum solvent model *J. Mol. Biol.* **303** 567–82
[64] Bensimon A, Simon A J, Chiffaudel A, Croquette V, Heslot F and Bensimon D 1994 Alignment and sensitive detection of DNA by moving interface *Science* **265** 2096–8
[65] Thundat T, Allison D P and Warmack R J 1994 Stretched DNA structures observed with atomic force microscopy *Nucleic Acids Res.* **22** 4224–8
[66] Weier H-U G, Wang M, Mullikin J C, Zhu Y, Cheng J-F, Greulich K M, Bensimon A and Gray J M 1995 Quantitative DNA fiber mapping *Hum. Mol. Genet.* **4** 1903–10
[67] Michalet X, Ekong R, Fougerousse F, Rousseaux S, Schurra C, Povey S, Beckmann J S and Bensimon A 1997 Dynamic molecular combing: stretching the whole human genome for high resolution studies *Science* **277** 1518–23
[68] Herrick J and Bensimon A 1999 Single molecule analysis of DNA replication *Biochimie* **81** 859–71
[69] Konrad M W and Bolonick J I 1996 Molecular dynamics simulation of DNA stretching is consistent with the tension observed for extension and strand separation and predicts a novel ladder structure *J. Am. Chem. Soc.* **118** 10 989–94
[70] Zhou H J and Zhang Y 2001 Pulling hairpinned polynucleotide chains: does base-pair stacking interaction matter *J. Chem. Phys.* **114** 8694–700
[71] Wilkins M H F, Gosling R G and Seeds W E 1951 Nucleic acid: an extensible molecule? *Nature* **167** 759–60
[72] Greenall R J, Nave C and Fuller W 2001 X-ray diffraction from DNA fibres under tension *J. Mol. Biol.* **305** 669–72
[73] Léger J F, Romano G, Sarkar A, Robert J, Bourdieu L, Chatenay D and Marko J F 1999 Structural transitions of a twisted and stretched DNA molecule *Phys. Rev. Lett.* **83** 1066–9
[74] Clausen–Schaumann H, Rief M, Tolksdorf C and Gaub H E 2000 Mechanical stability of single DNA molecules *Biophys. J.* **78** 1997–2007
[75] Williams M C, Wenner J R, Rouzina I and Bloomfield V A 2001 Effect of pH on the overstretching transition of double-stranded DNA: evidence of force-induced DNA melting *Biophys. J.* **80** 874–81
[76] Boland T and Ratner B D 1995 Direct measurement of hydrogen bonding in DNA nucleotide bases by atomic force microscopy. *Proc. Natl Acad. Sci. USA* **92** 5297–301
[77] Bustamante C, Smith S B, Liphardt J and Smith D 2000 Single-molecule studies of DNA mechanics *Curr. Opin. Struct. Biol.* **10** 279–85
[78] Krautbauer R, Clausen–Schaumann H and Gaub H 2000 Cisplatin changes the mechanics of single DNA molecules *Angew. Chem. Int. Edn* **39** 3912–5
[79] Strunz T, Oroszlan K, Schafer R and Guntherdort H J 1999 Dynamic force spectroscopy of single DNA molecules *Proc. Natl Acad. Sci. USA* **96** 11 277–82
[80] Lebrun A and Lavery R 1996 Modeling the mechanics of a DNA oligomer *J. Biomol. Struct. Dyn.* **16** 593–604
[81] Lavery R and Lebrun A 1999 Modelling DNA stretching for physics and biology *Genetica* **106** 75–84
[82] Strick T, Croquette V and Bensimon D 1998 Homologous pairing in streched supercoiled DNA *Proc. Natl Acad. Sci. USA* **95** 10 579–83
[83] Allemand J-F, Bensimon D, Lavery R and Croquette V 1998 Stretched and overwound DNA forms a Pauling-like structure with exposed bases *Proc. Natl Acad. Sci. USA* **95** 14152–7
[84] White J H 1969 Self linking and the Gauss integral in higher dimensions *Am. J. Math.* **91** 693–728
[85] Hagerman P J 1988 Flexibility of DNA *Annu. Rev. Biophys. Biophys. Chem.* **17** 265–8
[86] Shore D and Baldwin R L 1983 Energetics of DNA twisting. I. Relation between twist and cyclization probability *J. Mol. Biol.* **170** 957–81
[87] Boles T C, White J H and Cozzarelli M R 1990 Structure of plectonemically supercoiled DNA *J. Mol. Biol.* **213** 931–51
[88] Bednar J, Furrer P, Stasiak A, Dubochet J, Egelman E and BatetSrich A 1994 The twist, writhe and overall shape of supercoiled DNA change during counterion-induced transition from a loosely to a tightly interwound superhelix *J. Mol. Biol.* **235** 825–47

[89] Selvin P R, Cook D N, Pon N G, Bauer W R, Klein M P and Hearst J E 1992 Torsional rigidity of positively and negatively supercoiled DNA *Science* **255** 82–5
[90] Declais A C, de la Tour C B and Duguet M 2001 Reverse gyrases from bacteria and archaea *Methods Enzymol.* **334** 146–62
[91] Bouchiat C and Mézard M 1998 Elasticity theory of a supercoiled DNA molecules *Phys. Rev. Lett.* **80** 1556–9
[92] Moroz J D and Nelson P 1998 Entropic elasticity of twist-storing polymers *Macromolecules* **31** 6333–47
[93] Pauling L and Corey R B 1953 A proposed structure for the nucleic acids *Proc. Natl Acad. Sci. USA* **39** 84–97
[94] Liu D J and Day L A 1994 Pf1 virus structure: helical coat protein and DNA with paraxial phosphates *Science* **265** 671–4
[95] Lavery R 1994 Modeling nucleic acids: fine structure, flexibility and conformational transitions *Adv. Comput. Biol.* **1** 69–145
[96] Lavery R, Zakrzewska K and Sklenar H 1995 JUMNA (junction minimization of nucleic acids) *Comput. Phys. Commun.* **91** 135–58
[97] Smith S B 1998 Twisting DNA molecules *Biophys. J.* **74** 1609–10
[98] Strick T R, Croquette V and Bensimon D 2000 Single-molecule analysis of DNA uncoiling by a type II topoisomerase *Nature* **404** 901–4
[99] Maier B, Bensimon D and Croquette V 2000 Replication by a single DNA-polymerase of a stretched single strand DNA *Proc. Natl Acad. Sci. USA* **97** 12 002–7
[100] Marko J F and Siggia E 1995 Stretching DNA *Macromolecules* **28** 8759–70
[101] Vologodskii A and Marko J F 1997 Extension of torsionally stressed DNA by external force *Biophys. J.* **73** 123–32
[102] Nelson P 1999 Transport of torsional stress in DNA *Proc. Natl Acad. Sci. USA* **96** 14 342–7
[103] Viovy J-L, Heller C, Caron F, Cluzel P and Chatenay D 1994 Ultrafast sequencing of DNA by mechanical opening of the double helix: a theoretical investigation *C. R. Acad. Sci., Paris* **317** 795–800
[104] Thompson R E and Siggia E D 1995 Physical limits on the mechanical measurement of the secondary structure of bio-molecules *Europhys. Lett.* **31** 335–40
[105] Bockelmann U, Essevaz-Roulet B and Heslot F 1998 DNA strand separation studied by single molecule force measurements *Phys. Rev.* E **58** 2386–94
[106] Breslauer K J, Frank R, Blöcker H and Marky L A 1986 Predicting DNA duplex stability from the base sequence *Proc. Natl Acad. Sci. USA* **83** 3746–50
[107] Lubensky D K and Nelson D R 2000 Pulling pinned polymers and unzipping DNA *Phys. Rev. Lett.* **85** 1572–5
[108] Kellermayer M S Z, Smith S B, Granzier H L and Bustamante C 1997 Folding–unfolding transition in single titin molecules characterized with laser tweezers *Science* **276** 1112–6
[109] Tskhovrebova L, Trinic J, Sleep J A and Simmons R M 1997 Elasticity and unfolding of single molecules of the giant muscle protein titin *Nature* **387** 308–12
[110] Oberhauser A F, Marszalek P E, Erickson H P and Fernandez J M 1998 The molecular elasticity of the extracellular matrix protein tenascin *Nature* **393** 181–5
[111] Rief M, Gautel M, Schemmel A and Gaub H E 1998 The mechanical stability of immunoglobulin and fibronectin III domains in the muscle protein titin measured by atomic force microscopy *Biophys. J.* **75** 3008–14
[112] Carrion-Vazquez M, Marszalek P E, Oberhause A and Fernandez J M 1999 Atomic force microscopy captures length phenotypes in single proteins *Proc. Natl Acad. Sci. USA* **96** 11 288–92
[113] Carrion-Vazquez M, Oberhauser A F, Fowler S B, Marszalek P E, Broedel S E, Clarke J and Fernandez J M 1999 Mechanical and chemical unfolding of a single protein: a comparison *Proc. Natl Acad. Sci. USA* **96** 3694–9
[114] Krammer A, Lu H, Isralewitz B and Vogel V 1999 Forced unfolding of the fibonectin type III module reveals a tensile molecular recognition switch *Proc. Natl Acad. Sci. USA* **96** 1351–6
[115] Marszalek P E, Lu H, Li H, Carrion-Vazquez M, Oberhauser A F, Schulten K and Fernandez J M 1999 Mechanical unfolding intermediates in titin modules *Nature* **402** 100–3
[116] Oesterhelt F, Oesterhelt D, Pfeiffer M, Engel A, Gaub H E and Müller D J 2000 Unfolding pathways of individual bacteriorhodopsins *Science* **286** 143–6
[117] Labeit S and Kolmerer B 1995 Titins: giant proteins in charge of muscle ultrastructure and elasticity *Science* **270** 293–6
[118] Erickson H P 1993 Tenascin-c, tenascin-r and tenascin-x: a family of talented proteins in search of functions *Curr. Opin. Cell. Biol.* **5** 869–76
[119] McGough A M and Joseph R 1990 On the structure of erythrocyte sprectrin in partially expanded membrane skeletons *Proc. Natl Acad. Sci. USA* **87** 5208–12
[120] Rief M, Pascual J, Saraste M and Gaub H E 1999 Single molecule force spectroscopy of spectrin repeats: low unfolding forces in helix bundles *J. Mol. Biol.* **286** 553–61

[121] Lenne P F, Raae A J, Altmann S M, Saraste M and Horber J K H 2000 States and transitions during forced unfolding of a single spectrin repeat *FEBS Lett.* **476** 124–8
[122] Lu H and Schulten K 2000 The key event in force induced unfolding of titin's immunoglobin domains *Biophys. J.* **79** 51–65
[123] Improta S, Politou A and Pastore A 1996 Immunoglobulin-like modules from titin i-band: extensible components of muscle elasticity *Structure* **4** 323–37
[124] Oberhauser A F, Marszalek P E, Erickson H P and Fernandez J M 1998 The molecular elasticity of the extracellular matrix protein tenascin *Nature* **393** 181–5
[125] Grigorieff N, Ceska T A, Downing K H, Baldwin J M and Henderson R 1996 Electron-crystallographic refinement of the structure of bacteriorhodopsin *J. Mol. Biol.* **259** 393–421
[126] Rief M, Oesterhelt F, Heymann B and Gaub H E 1997 Single molecule force spectroscopy on polysaccharides by atomic force microscopy *Science* **275** 1295–7
[127] Li H, Rief M, Oesterhelt F and Gaub H E 1998 Single force microscopy on xanthan by AFM *Adv. Matter* **3** 316–9
[128] Marszalek P E, Oberhauser A F, Pang P and Fernandez J M 1998 Polysaccharide elasticity governed by chair–boat transitions of the glucopyranose ring *Nature* **396** 661–4
[129] Li H, Rief M, Oesterhelt F, Gaub H E, Zhang X and Shen J 1999 Single-molecule force spectroscopy on polysaccharides by AFM—nanomechanical fingerprint of α-(1,4)-linked polysaccharides *Chem. Phys. Lett.* **305** 197–201
[130] Marszalek P E, Pang Y P, Li H, Yazal J E and Oberhauser A 1999 Atomic levers control pyranose ring conformations *Proc. Natl Acad. Sci. USA* **96** 7894–8
[131] Miyamoto S and Kollman P 1993 Absolute and relative binding free energy calculations of the interaction of biotin and its analogs with streptavidin using molecular dynamics/free energy perturbation approaches *Proteins* **16** 226–31
[132] Balsera M, Stepaniants S, Izrailev S, Oono Y and Schulten K 1997 Reconstructing potential energy functions from simulated force-induced unbinding processes *Biophys. J.* **73** 1281–7
[133] Merkel R, Nassoy P, Leung A, Ritchie K and Evans E 1999 Energy landscapes of receptor–ligand bonds explored with dynamic force spectroscopy *Nature* **397** 50–3
[134] Scwesinger F, Ros R, Strunz T, Anselmetti D, Güntherodt H J, Honegger A, Jermutus L, Tiefenauer L and Plückthun A 2000 Unbinding forces of single antibody–antigen complexes correlate with their thermal dissociation rates *Proc. Natl Acad. Sci. USA* **97** 9972–7